ICES Cooperative Research Report

Rapport des Recherches Collectives

No. 316

February 2013

ICES/GLOBEC workshop on long-term variability in southwestern Europe

Editor

Maria de Fátima Borges

Authors

Jürgen Alheit · Antonio Bode
Maria de Fátima Borges · Mª Luz Fernández de Puelles
Louize Hill · Alicia Lavín · Hugo Mendes
Manuel Ruiz-Villarreal · A. Miguel P. Santos · Raquel Somavilla
Andrés Uriarte · Victor Valencia · Manuel Vargas-Yáñez

ICES International Council for the Exploration of the Sea

CIEM Conseil International pour l'Exploration de la Mer

International Council for the Exploration of the Sea
Conseil International pour l'Exploration de la Mer

H. C. Andersens Boulevard 44–46
DK-1553 Copenhagen V
Denmark
Telephone (+45) 33 38 67 00
Telefax (+45) 33 93 42 15
www.ices.dk
info@ices.dk

Recommended format for purposes of citation:

Borges, M. F. (Ed). 2013. ICES/GLOBEC workshop on long-term variability in southwestern Europe. ICES Cooperative Research Report No. 316. 55 pp.

Series Editor: Emory D. Anderson

ISBN 978-87-7482-122-9

ISSN 1017-6195

Contents

Summary

Maria de Fátima Borges, Jürgen Alheit, Alicia Lavín, Andrés Uriarte, and Antonio Bode

The Workshop on Long-term Variability in Southwestern Europe (WKLTVSWE) was held in Lisbon, Portugal from 13 to 16 February 2007, a joint effort of ICES and GLOBEC and endorsed by EUR-OCEANS (http://www.eur-oceans.org). In 1997, GLOBEC's SPACC (Small Pelagic Fish and Climate Change) initiative held a joint meeting with SCOR Working Group 98 on worldwide, large-scale fluctuations in sardine (*Sardinops sagax*) and anchovy (*Engraulis* spp.) populations (Schwartzlose *et al.*, 1999). It was decided then to continue this "global" undertaking with a series of regional workshops. Previous meetings had focused on the Benguela Current in 2001 (Cury and Shannon, 2004), the Humboldt Current in 2002 (Alheit and Niquen, 2004), and Japanese waters in 2003. During the 2005 annual meeting of the former ICES Study Group on Regional Ecology of Small Pelagics (SGRESP)–subsequently ICES/GLOBEC Working Group on Life Cycle and Ecology of Small Pelagic Fish (WGLESP)–it was recommended that this series of workshops be continued with a meeting focusing on the waters surrounding the Iberian Peninsula, including the western Mediterranean Sea.

A synthesis of the hydrography, oceanography, and biology of southwestern European waters is presented. The goals of the workshop were to (i) provide a survey of large-scale, long-term changes throughout the ecosystems surrounding the Iberian Peninsula (are there signals of regime shifts in the region?), (ii) identify apparent synchronies (teleconnection patterns) with other regions of the North Atlantic or northern hemisphere, and (iii) gain insight into the causes and mechanisms underlying the major ecosystem changes, e.g. identify possible links of those changes in the ecosystems to climate variability. Testing materials were climatic and oceanographic variables, ecosystem indices (zooplankton and phytoplankton indices), and population indices of small pelagic (catches and recruitment series) in addition to climate-forcing indices at local and worldwide scales.

The time-series compiled during the workshop were as broad as possible. In all, 73 data time-series were compiled and classified by type: global climatic and biological indices. With the objective of identifying and analysing oscillations at multi-annual scale in the variability of the time-series, it was decided to work on three case studies: Case study 1 – global region, Atlantic Iberian Peninsula; Case study 2 – local region, Portugal; Case study 3 – local region, Bay of Biscay.

The results of the global case study revealed significant interannual trends in climate, oceanographic, and ecosystem variables, regional indications of global warming since ca. 1950. Quasi-decadal scales are characteristic of climate, oceanographic, and fish abundance indices, but plankton indices are over shorter periods. Sardine and anchovy demonstrated synchrony in positive and negative phases up to 1978, increasing and decreasing simultaneously. This pattern was broken and moved to asynchrony thereafter, when sardine and anchovy were in opposite phase. The Portuguese case study demonstrates that sardine catches are negatively correlated with northwesterly winds, and that these are strongly and positively correlated with the North Atlantic Oscillation (NAO). Sardine catches exhibited periods of 20–29 years, and ten years of cyclic variation. The Bay of Biscay case study demonstrated that anchovy recruitment is significantly correlated with local downwelling and

upwelling events that can be measured at 45°N 2°W, and that it follows a seasonal pattern. During winter, the water column has almost no stratification as a result of convergence and downwelling from western poleward currents bringing warmer, more-saline water of subtropical origin. During summer, water-column stratification increases when northerly winds dominate and mechanisms of divergence and stable stratification prevail, bringing colder, less-saline water of subpolar origin to the Bay of Biscay. This weak upwelling yields stable stratification that favours good recruitment. Nevertheless, if spring–summer northerly winds induce gales and storms, disrupting stable stratification, this would be detrimental to anchovy success. A general mechanism emerged, of an alternation of periodical quasi-decadal dominance of boreal fresher, colder water and subtropical warmer, more-saline water. In accordance with the biogeography of the region, this seems to favour the productivity of each species differently.

1 Introduction

Jürgen Alheit, Maria de Fátima Borges, Alicia Lavín, Andrés Uriarte, and Antonio Bode

Understanding the role of natural variability over a variety of time-scales is essential if one is to manage marine living resources effectively. Evidence exists that marine ecosystems undergo large-scale, decadal fluctuations that seem to be driven by climate forcing (Stenseth *et al.*, 2002), as clearly demonstrated for the North Sea and the Baltic Sea (Beaugrand, 2004; Alheit *et al.*, 2005), the North Pacific (Hare and Mantua, 2000), and eastern boundary current systems (Chavez *et al.*, 2003; Alheit and Niquen, 2004). Shifts in climate regimes can change marine communities and trophodynamic relationships and induce changes in the mix of dominating species over decadal time-scales. Evidence of such shifts was gained largely through retrospective studies, i.e. the analyses of historical atmospheric and marine data. In some instances, palaeorecords have allowed us to look farther back in time and, most importantly, at periods when human intervention through fishing was not as important as it is today. The impact of climate variability on marine ecosystems has been the focus of a number of national and international regional projects carried out in local waters through a combination of retrospective investigations, modelling efforts, and process studies. GLOBEC workshops have concentrated on ecosystems in which small pelagic fish, such as anchovy and sardine, are important, along with horse mackerel (*Trachurus trachurus*). Reasons for this are (Hunter and Alheit, 1995):

- Small pelagic fish such as sardine, anchovy, herring (*Clupea harengus*), sprat (*Sprattus sprattus*), and others represent ca. 20–25% of the total annual world fisheries catch.
- They are widespread and in all oceans.
- They support important fisheries all around the world, and the economies of many countries depend on their fisheries.
- They respond dramatically and quickly to changes in ocean climate.
- Most species are highly mobile, have short, plankton-based food chains, and some even feed directly on phytoplankton.
- They are short-lived (3–7 years), highly fecund, and can spawn year-round (many of them do so).
- These biological characteristics make them very sensitive to environmental forcing and highly variable in their abundance (Hunter and Alheit, 1995).
- Thousand-fold changes in abundance over a few decades are characteristic for small pelagics, well-known examples including the Japanese sardine (*Sardinops melanostictus*), the sardine in the California and Benguela Currents (*Sardinops sagax*), anchovy (*Engraulis ringens*) in the Humboldt Current, anchovy in the Benguela Current (*Engraulis encrasicolus*), and herring in European waters.
- Their drastic stock fluctuations often have dramatic consequences for fishing communities, entire regions, and even whole countries.
- Their dynamics have important economic consequences as well as ecological ones.

- They are the forage for larger fish, seabirds, and marine mammals. The collapse of small pelagic fish populations is often accompanied by sharp declines in seabird and marine mammal populations that depend on them for food.
- Major changes in the abundance of small pelagic fish may be accompanied by marked changes in ecosystem structure. They are often accompanied by rigorous changes in abundance and species composition of zooplankton.
- The great plasticity in the growth, survival, and other life-history characteristics of small pelagic fish is key to their dynamics and makes them ideal targets for testing the impact of climate variability on marine ecosystems and fish populations and, in general, marine ecosystems.

Valuable accounts of long-term changes in anchovy and sardine and their respective ecosystems around the Iberian Peninsula and the potential impact of climate variability have been published recently (Borja *et al.*, 1998; Allain *et al.*, 2001; Uriarte *et al.*, 2002; Borges *et al.*, 2003; Guisande *et al.*, 2004; Bode *et al.*, 2006). However, those studies concentrated on single species or ecosystems and were restricted to regional parts of southwestern European waters. The report of this workshop is meant to analyse long-term time-series of physical and biological data from the seas surrounding the Iberian Peninsula in a comparative manner, focusing on long-term changes in small pelagic fish, to enhance understanding of the response of marine ecosystems to low-frequency environmental change and improve knowledge of the impact of climate variability on marine ecosystems.

The comparative approach was chosen to elucidate the mechanisms controlling the abundance and distribution of marine populations. Improved mechanistic understanding of the coupling between physics and biology will, in turn, likely make it possible to improve the reliability of predictions of the future composition of marine communities and provide a fresh basis for ecosystem and resource management.

2 Southwestern European waters

2.1 Southern Atlantic waters

A. Miguel P. Santos, Alicia Lavín, Manuel Ruiz-Villarreal, Victor Valencia, Louize Hill, Andrés Uriarte, and Maria de Fátima Borges

Most of the water masses in the region (Figure 2.1) are of North Atlantic origin, including those that have been transformed after mixing with Mediterranean water. The region is affected by both subpolar and subtropical gyres, depending on latitude, but the general circulation in the area follows the subtropical anticyclonic gyre in a relatively weak manner (1–2 cm s^{-1}). The southern part of the Bay of Biscay along the northern Spanish coast is known as the Cantabrian Sea and is characterized by a narrow shelf. Farther south, a narrow shelf continues west, off Portugal. Lastly, to the south, the Gulf of Cádiz has a wider shelf that is strongly influenced by the Mediterranean Sea. Within these zones, the topographic diversity and wide range of substrata result in many different types of coastal habitat (OSPAR, 2000).

The eastern boundary of the North Atlantic subtropical gyre extends from the northern tip of the Iberian Peninsula at 43°N to south of Senegal at ca. 10°N, approximately the displacement of the trade-wind band. The meridional shift in the trade-wind system causes seasonal upwelling at the extremes of the band, whereas in the central region, upwelling is relatively continuous year-round (Wooster *et al.*, 1976; Arístegui *et al.*, 2004).

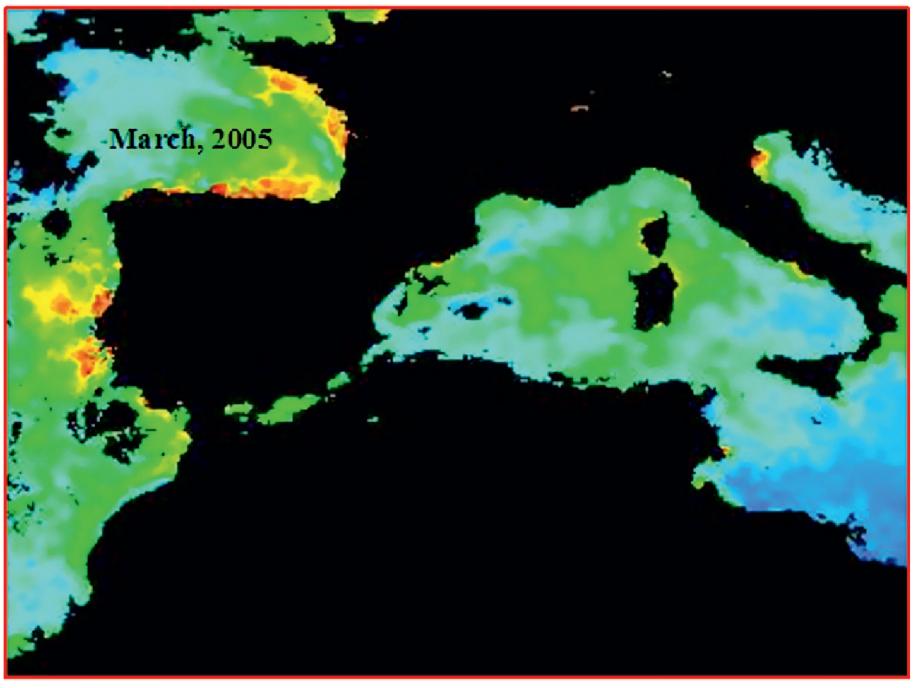

Figure 2.1. March 2005 map showing the waters around the Iberian Peninsula, including the Bay of Biscay, the Cantabrian Sea, Portuguese continental waters, the Gulf of Cádiz, and the Mediterranean Sea.

Superimposed on the seasonal variation, short-term variability of wind direction and intensity may induce or suppress upwelling, affecting the dynamics of the ecosystem. The upwelling region is separated into two distinct areas, the Iberian coast and the

northwest African coast, with apparently little continuity in the flow between them. This is caused by the interruption of the coastline at the Strait of Gibraltar, which funnels the exchange of water between the Mediterranean Sea and the Atlantic Ocean. Associated with the topography of the shelf, large filaments of coastal upwelled water stretch offshore from the numerous capes and promontories, exchanging water and biological properties with the ocean boundary. This exchange is particularly noticeable along the giant filaments of Cape Cuir and Cape Blanc, which stretch up to several hundred kilometres into the open ocean, transporting water rich in organic matter (Arístegui *et al.*, 2004).

In the Cantabrian Sea, surface currents generally flow east during winter and spring and west in summer, following windforcing (Lavín *et al.*, 2005). The changes in the direction of the currents produce seasonal coastal upwelling. The circulation on the west coast of the Iberian Peninsula is characterized by a complex current system subject to strong seasonality and mesoscale variability, demonstrating reversing patterns between summer and winter in the upper layers of the slope and over the outer shelf (Barton, 1998; Peliz *et al.*, 2005; Ruiz-Villarreal *et al.*, 2006). During spring and summer, northerly winds blowing along the coast dominate, causing coastal upwelling and producing a south-flowing current at the surface and a north-flowing undercurrent at the slope (Fiúza *et al.*, 1982; Haynes and Barton, 1990; Peliz *et al.*, 2005; Mason *et al.*, 2006).

In autumn and winter, the surface circulation is predominantly northward, partially driven by meridional alongshore density gradients (Peliz *et al.*, 2003a, 2003b), and transporting warmer (subtropical) water of higher salinity over the shelf break (Frouin *et al.*, 1990; Haynes and Barton, 1990; Pingree and Le Cann, 1990) – the Iberian Poleward Current (Peliz *et al.*, 2003b). These waters are nutrient-poor and contribute to fronts that determine the distribution of plankton, and of fish eggs and larvae (Fernández *et al.*, 1993; González-Quirós *et al.*, 2003). Strong subtropical water intrusions in the Cantabrian Sea may be a feature strongly influenced by wind events (Villamor *et al.*, 2005). Another important feature of the upper layer is the Western Iberia Buoyant Plume (WIBP; Peliz *et al.*, 2002), which is a low-salinity, surface-water body fed by winter-intensified run-off from several rivers from the northwest coast of Portugal and the Galician Rias. The WIBP could play an important role in the survival of fish larvae (Santos *et al.*, 2004).

The intermediate layers are occupied mainly by a poleward flow of Mediterranean Water (MW), which tends to contour the southwestern slope of the Iberian Peninsula (Ambar and Howe, 1979), generating mesoscale features known as meddies (Serra and Ambar, 2002), which can transport saline, warm MW over great distances. The exchange of water masses through the Strait of Gibraltar is driven by the deep, very saline (S >37), warm Mediterranean Outflow Water (MOW) that flows into the Gulf of Cádiz, and the less-saline, cool-water mass of Atlantic Intermediate Water (AIW) at the surface. The most important features enhancing primary production are coastal upwelling, coastal run-off, river plumes, seasonal currents, internal waves, and tidal fronts. Water temperature is highest in the south, where it is influenced by the MW. For example, the annual mean temperature at 100 m is 11.2°C north of the region (48°N), and 15.6 °C to the south (36°N; Conkright *et al.*, 2002).

Upwelling events are a common feature in Portugal, west of Galicia, and in a narrow coastal band in the western Cantabrian Sea, especially in summer (Fraga, 1981; Fiúza *et al.*, 1982; Blanton *et al.*, 1984; Botas *et al.*, 1990; OSPAR, 2000). The climate and oceanographic features of the inner part of the Bay of Biscay follow the main trends

and patterns described above for the Iberian Atlantic coasts at the intergyre region of the northeastern Atlantic Ocean (Valencia *et al.*, 2003). Eastern North Atlantic Central Water (ENACW) is the main water mass in the upper layers of the Bay of Biscay; it occupies almost all of the water volume over the continental shelf and slope. However, the upper layers suffer some modifications (at regional and seasonal scales) caused largely by the close coupling of meteorological and oceanographic data in the inner part of the Bay of Biscay (Pérez *et al.*, 1995, 2000; Valencia *et al.*, 2003) and shown by, for instance, the relationships between atmospheric temperature, sea surface temperature (SST), heat content, and salinity, in relation to the balance of precipitation minus evaporation and the influence of river flows.

In this region, two varieties of ENACW can be identified: colder, fresher ENACWP of subpolar origin, and warmer, more-saline ENACWT of subtropical origin (Ríos *et al.*, 1992). The relative occurrence of those water masses in the southeastern Bay of Biscay, as well as the extent of modification of their characteristics, is related to the main seasonal cycle and to the specific climate conditions. During autumn and winter, southerly and westerly winds dominate and a poleward current prevails, with associated mechanisms of convergence, downwelling, and vertical mixing. During spring and summer, southerly and westerly winds are less dominant, and northeasterly winds prevail, with associated mechanisms of divergence, upwelling, and stable stratification. This regimen also increases the proportion of relatively colder, less-saline water (ENACWP) into the southeastern Bay of Biscay in summer (Valencia *et al.*, 2004).

The seasonal interplay of the large-scale climatology between the Azores high-pressure cell, which is strong and displaced northwards during summer, and the Icelandic low, which weakens then, governs the setup of favourable upwelling winds (northerlies) off western Iberia between April and October (Wooster *et al.*, 1976; Fiúza *et al.*, 1982). During winter, the dominant wind direction changes, and poleward flow becomes a conspicuous feature at all levels between the surface and the MW at ~1500 m along the Iberian shelf edge and slope. The surface poleward current carries relatively warm, saline water clearly identifiable in SST satellite imagery (Frouin *et al.*, 1990; Haynes and Barton, 1990; Peliz *et al.*, 2005) that propagates to locations as far north as the Cantabrian Sea (Pingree and Le Cann, 1990) and Goban Spur, northwest of the United Kingdom at the continental margin (Pingree, 1993).

For the North Atlantic system, the Canary and Iberian regions form two different subsystems (Barton, 1998). The separation is not simply geographic, but a consequence of the discontinuity imposed by the strait at the entrance to the Mediterranean Sea, allowing the exchange between two different water masses with a profound impact on regional circulation (Relvas *et al.*, 2006). The latter author suggests that large-scale climatological patterns are partly obscured by mesoscale activity.

The upper waters of the Bay of Biscay have experienced progressive warming during the past and present centuries. Mean SSTs increased by 1.48°C in the southeastern Bay of Biscay over the period 1972–1993 (0.68°C per decade) and by 1.038°C over the past century (Koutsikopoulos *et al.*, 1998; Planque *et al.*, 2003). The increase in heat content stored in the water column appears to be greatest in the 200–300 m layer (González-Pola and Lavín, 2003), and it is in this layer that the ENACW responds quickly to climate forcing in areas of water-mass formation located in the northern Bay of Biscay and adjacent areas. In the southern Bay of Biscay in the ENACW, temperature increased during the past decade by 0.032°C year^{-1}, and in the

Mediterranean Water by ~0.020°C and by 0.005 for salinity (González-Pola *et al.*, 2005).

2.2 Balearic Sea

Mª Luz Fernández de Puelles

The Balearic Islands in the central western Mediterranean basin represent a complex topographic barrier separating two sub-basins in which there are different water masses. The marine region can be considered as a transition zone where water masses of southern and northern origin meet in the surface layer (0–100 m). In the northwestern Mediterranean, the Balearic Sea receives cold, saline water originating during winter in the Gulf of Lions, where strong winds are frequent; in the south, the Alborán basin, where weather conditions are milder, is the direct receptor of Atlantic waters through Gibraltar of warmer, less-saline water. Therefore, in the Balearic Sea and particularly in its channels, cool, saline northern waters proceeding north encounter warmer, fresher water of Atlantic origin flowing north (Font *et al.*, 1988; García *et al.*, 1994; Pinot *et al.*, 1994). The Mallorca Channel is the preferred route of southern waters in their northward spread. Nevertheless, the circulation can be reversed during winter and spring as cool, south-flowing water of northern origin (Pinot *et al.*, 2002). According to the time of year and the mesoscale processes in adjacent areas, these waters mix, but there are also clear inputs of different water masses, forming frontal systems with more or less similar intensity and permanence (Lopez-Jurado, 2002). During the period 1994–2003, interannual variability in the hydrography of the islands was high and the main driver of zooplankton variability (Fernández de Puelles *et al.*, 2004a). However, northern, more-saline water flowing south is more common in winter; during autumn, Atlantic water flowing north is more prevalent. Permanent mesoscale eddies disturb the area, resulting in characteristic complex circulation patterns. The seasonal and interannual variability of these currents has been investigated during the past decade by oceanographers investigating their relationship to atmospheric forcing, but the implication on planktonic communities is still poorly understood (Fernández de Puelles *et al.*, 2004b). Multidisciplinary projects since 1994 have found that the Mallorca Channel is a good place for long-term monitoring, particularly of the boundary character of the area, where any hydrographic change can be reflected by the zooplankton community (Fernández de Puelles *et al.*, 2004a). In addition, the area is not affected by river discharge or pollutants of terrestrial origin, and is more influenced by ocean than by coastal circulation, such as that at play over shelf areas, where there tends to have been more research (Estrada *et al.*, 1985). Considering the above, the Channel could well represent the transitional open-sea environment of the Mediterranean pelagic ecosystem.

3 Data

Antonio Bode, Alicia Lavín, Raquel Somavilla, Victor Valencia, Andrés Uriarte, Hugo Mendes, Maria de Fátima Borges, and A. Miguel P. Santos

In all, 73 climatic, oceanographic, and biological variables were identified, and the data for each of these variables have been identified. The longest available time-series was from 1940 to 2005 for variables such as the North Atlantic Oscillation (NAO) index, the Global Temperature Anomaly, the Portuguese north wind, or sardine landings. Shorter time-series were available for other variables, the shortest being for anchovy and horse mackerel recruitment in the Bay of Biscay, which was only from 1986 and 1985, respectively, to 2005.

The time-series used in the workshop were as broad as possible and include different types of climatological, oceanographic, and biological data to cover most of the variability of the area. The period studied in the long-term analyses was fixed at 1960–2005. Short-term data series were also computed to evaluate regional variability. Tables 3.1–3.3 summarize the 73 variables, show the period for which data are available, and list the data sources. The variables are organized according to abiotic and biotic data type: global climate, physical oceanographic, and biological indices.

3.1 Global climatic indices

Table 3.1. The 17 available time-series of global climate indices and the sources of data.

No.	Variable	Definition	Start–end	Source of data
1	NAO	North Atlantic Oscillation	1950 – 2005	PFEL-NOAA. Annual standardized means from PCA monthly values
2	EA	Eastern Atlantic pattern	1950 – 2005	PFEL-NOAA. Annual standardized means from PCA of monthly values
3	WP	Western Pacific pattern	1950 – 2005	PFEL-NOAA. Annual standardized means from PCA monthly values
4	EP_NP	Eastern Pacific/North Pacific pattern	1950 – 2005	PFEL-NOAA. Annual standardized means from PCA monthly values
5	PNA	Pacific North American pattern	1950 – 2005	PFEL-NOAA. Annual standardized means from PCA monthly values
6	EA_WR	East Atlantic/West Russia pattern	1950 – 2005	PFEL-NOAA. Annual standardized means from PCA monthly values
7	SCA	Scandinavia pattern	1950 – 2005	PFEL-NOAA. Annual standardized means from PCA monthly values
8	TNH	Tropical/Northern hemisphere pattern	1950 – 2005	PFEL-NOAA. Annual standardized means from PCA monthly values
9	POL	Polar/Eurasia pattern	1950 – 2005	PFEL-NOAA. Annual standardized means from PCA monthly values
10	PT	Pacific Transition pattern	1950 – 2005	PFEL-NOAA. Annual standardized means from PCA monthly values
11	CLI1	1st PCA component of climate indices	1950 – 2005	PCA of teleconnection indices
12	CLI2	2nd PCA component of climate indices	1950 – 2005	PCA of teleconnection indices
13	CLI3	3rd PCA component of climate indices	1950 – 2005	PCA of teleconnection indices
14	NAO_DM	North Atlantic Oscillation (Hurrell, 1995) December–March	1940 – 2005	Climate Research Unit (CRU) actual values (not from PCA components)
15	NAO_m	North Atlantic Oscillation (Hurrell, 1995) annual mean	1940 – 2005	Climate Research Unit (CRU) actual values (not from PCA components)

No.	Variable	Definition	Start–end	Source of data
16	At_global	Global temperature anomaly (continent–ocean) from mean value between 1880 and 2000 (°C)	1940–2005	Climate Research Unit (CRU)
17	At_NH	Northern hemisphere temperature anomaly (continent–ocean) from mean value between 1880 and 2000 (°C)	1940–2005	Climate Research Unit (CRU)

3.2 Physical oceanographic indices

Table 3.2. The 29 available time-series for local physical oceanographic indices and the sources of data.

No.	Variable	Definition	Start–end	Source of data
18	AMO	Atlantic Multidecadal Oscillation (SST anomaly from detrended mean global warming value)	1940–2005	Climate Data Center (CDC), NOAA
19	SSTP	Mean SST, Portugal (39.5°N 09.5°W, °C)	1960–2002	ICOADS (reanalysis data) 2° × 2° grid
20	RFG	Mean annual river flow, Gironde (Garonne+Dordogne, $m^3 s^{-1}$)	1952–2005	AZTI from various sources
21	SSTSS	Mean SST at San Sebastian Aquarium (°C)	1947–2005	AZTI from various sources
22	POLE	Poleward index at 43°N 11°W from geostrophic winds (quarterly, October–December of preceding year)	1955–2004	Cabanas (2000)
23	Uls_4311	Upwelling index at 43°N 11°W from geostrophic winds (March–October, $m^3 s^{-1} km^{-1}$)	1966–2005	Lavín *et al.* (1991)
24	Uim_4311	Upwelling index at 43°N 11°W from geostrophic winds (annual mean, $m^3 s^{-1} km^{-1}$)	1966–2005	Lavín *et al.* (1991)
25	TPEA	Mean water transport from potential energy anomaly, North Atlantic (Mt s^{-1})	1955–2005	WHOI, Ruth Curry
26	SST_4503	Mean SST (45°N 03°W, °C)	1955–2005	ICOADS
27	SST_4311	Mean SST (43°N 11°W, °C)	1955–2005	R. Somavilla and A. Lavín (pers. comm.)
28	TAIR_4311	Mean air temperature (43°N 11°W, °C)	1955–2005	R. Somavilla and A. Lavín (pers. comm.)
29	U_4503	Mean E–W wind (45°N 03°W, m s^{-1})	1955–2005	R. Somavilla and A. Lavín (pers. comm.)
30	V_4503	Mean N–S wind (45°N 03°W, m s^{-1})	1955–2005	R. Somavilla and A. Lavín (pers. comm.)
31	U_4311	Mean E–W wind (43°N 11°W, m s^{-1})	1955–2005	R. Somavilla and A. Lavín (pers. comm.)
32	V_4311	Mean N–S wind (43°N 11°W, m s^{-1})	1955–2005	R. Somavilla and A. Lavín (pers. comm.)
33	NWPw	North wind, Portugal (40°N 10°W, January–March, m s^{-1})	1940–2000	R. Somavilla and A. Lavín (pers. comm.)
34	NWPs	North wind, Portugal (40°N 10°W, June–Aug, m s^{-1})	1940–2000	NCAR reanalysis data (original data from 5° × 5° grid, 30–50°N 25–5°W)
35	SOFWE	Significantly offshore favourable wind events, Portugal (number of events with >4 favourable days)	1948–2003	H. Mendes (pers. comm.)
36	SUFWE	Significantly upwelling favourable wind events, Portugal (number of events with >4 favourable days)	1948–2003	H. Mendes (pers. comm.)
37	HSFWE	Hybrid SUFWE-SOFWE events, Portugal	1948–2003	H. Mendes (pers. comm.)
38	SONFWE	Significantly onshore favourable wind events, Portugal (number of events with >4 favourable days)	1948–2003	H. Mendes (pers. comm.)
39	UILm_4502	Upwelling index, Landes (45°N 02°W, annual mean, $m^3 s^{-1} km^{-1}$)	1967–2005	ICOADS (reanalysis data) 2°×2° grid
40	UIBm_4502	Upwelling index, Basque coast (45°N 02°W, annual mean, $m^3 s^{-1} km^{-1}$)	1967–2005	ICOADS (reanalysis data) 2°×2° grid

No.	Variable	Definition	Start – end	Source of data
41	UIBs_4502	Upwelling index, Basque coast (45 °N 2 °W, annual mean of positive values, March–July, $m^3 s^{-1} km^{-1}$)	1967 – 2005	V. Valencia and A. Borja (pers. comm.)
42	TURB_4502	Mean annual turbulence, Bay of Biscay (at 45 °N 02 °W, $m^3 s^{-1}$)	1967 – 2005	ICOADS (reanalysis data) 2 °×2 ° grid
43	SHF_4503	Annual mean sensible heat fluxes, Bay of Biscay (45 °N 03 °W, W m^{-2})	1948 – 2005	ICOADS (reanalysis data) 2 °×2 ° grid
44	LHF_4503	Annual mean latent heat fluxes, Bay of Biscay (45 °N 03 °W, W m^{-2})	1948 – 2005	ICOADS (reanalysis data) 2 °×2 ° grid
45	ZMF_4503	Annual mean zonal momentum flux, Bay of Biscay (45 °N 03 °W, N m^{-2})	1948 – 2005	ICOADS (reanalysis data) 2 °× 2 ° grid
46	MMF_4503	Annual mean meridional momentum flux, Bay of Biscay (45 °N 03 °W, N m^{-2})	1948 – 2005	ICOADS (reanalysis data) 2 °× 2 ° grid

3.3 Biological indices

The available biological indices for the Iberian region are listed in Table 3.3. They include landings and recruitment data for sardine, anchovy, and horse mackerel from the different Iberian subareas.

Phytoplankton colour index (PCI) time-series observed in Galicia–Portugal and in the Bay of Biscay monitored by the Continuous Plankton Recorder (CPR) provided by SAFHOS (http://www.sahfos.org/) were available between 1958 and 2004. Mesozooplankton biomass and copepod abundance time-series of several local subareas were the basis for biological indicators of ecological processes, e.g. the phytoplankton–zooplankton index (PZI).

Table 3.3. The 26 available biological time-series indices: description, period, and sources of data.

No.	Variable	Definition	Start–end	Source of data
47	sard_PNW	Sardine landings (×1000 t), ICES, NW Portugal	1940 – 2005	Mendes and Borges (2006)
48	sard_PSW	Sardine landings (×1000 t), ICES, SW Portugal	1940 – 2005	Mendes and Borges (2006)
49	sard_PS	Sardine landings (×1000 t), ICES, S Portugal	1940 – 2005	Mendes and Borges (2006)
50	sard_PW	Sardine landings (×1000 t), ICES, SW Portugal = sard_PNW+sard_PSW	1940 – 2005	Mendes and Borges (2006)
51	sard_P	Sardine landings (×1000 t), ICES, Portugal = sard_PNW+sard_PSW +sard_PS	1940 – 2005	Mendes and Borges (2006)
52	anch_BBI	Anchovy landings (×1000 t), ICES Divisions VIIIa,b,c (France+Spain)	1940 – 2005	ICES; A. Uriarte (pers. comm.)
53	anch_BBS	Anchovy landings (×1000 t), ICES Divisions VIIIb,c (Spain)	1940 – 2005	ICES; A. Uriarte (pers. comm.)
54	sardine	Sardine landings (×1000 t), ICES Divisions VIIIc+IXa	1940 – 2005	ICES; A. Bode (pers. comm.)
55	anchovy	Anchovy landings (×1000 t), ICES Divisions VIIIc+IXa	1943 – 2005	ICES; A. Bode (pers. comm.)
56	sard_e	Sardine landings (standardized, normalized, detrended)	1940 – 2005	A. Bode (pers. comm.)
57	anch_e	Anchovy landings (standardized, normalized, detrended)	1943 – 2005	A. Bode (pers. comm.)
58	RIS	Regime indicator series = sard_e - anch_e	1940 – 2005	A. Bode (pers. comm.)
59	ARI	Anchovy recruitment index (ICES Subarea VIII; relative units)	1967 – 2003	ICES; A. Uriarte (pers. comm.)

No.	Variable	Definition	Start–end	Source of data
60	AR	Anchovy recruitment (Bay of Biscay, ICES Subarea VIII; no. × 10^9)	1986 – 2005	ICES; A. Uriarte (pers. comm.)
61	SR	Sardine recruitment (Iberia, ICES Divisions VIIIc+IXa; no. × 10^9)	1978 – 2004	ICES; A. Uriarte (pers. comm.)
62	HMRI	Horse mackerel recruitment (Iberia, ICES; no. × 10^9)	1985 – 1999	ICES; A. Uriarte (pers. comm.)
63	HMR	Horse mackerel recruitment (European Atlantic, ICES; no. × 10^9)	1982 – 2004	ICES; A. Lavín; P. Abaunza (pers. comm.)
64	PCI_F4	Phytoplankton colour index (from CPR); annual mean, area F4 (Galicia–Portugal)	1958 – 2004	Continuous Plankton Recorder (CPR, SAHFOS)
65	PCI_E4	Phytoplankton colour index (from CPR); annual mean, area E4 (Bay of Biscay)	1958 – 2004	Continuous Plankton Recorder (CPR, SAHFOS)
66	COP_F4	Copepod abundance (from CPR; no. × 10^3 $(3\ m^3)^{-1}$), area F4	1958 – 2004	Continuous Plankton Recorder (CPR, SAHFOS)
67	COP_E4	Copepod abundance (from CPR; no. × 10^3 $(3\ m^3)^{-1}$), area E4	1958 – 2004	Continuous Plankton Recorder (CPR, SAHFOS)
68	DWCPR	Mesozooplankton biomass (mg DW m^{-3}) estimated from abundance for E4+F4 CPR areas	1958 – 2003	A. Lopez-Urrutia (pers. comm.)
69	PCI_m	Phytoplankton colour index (from CPR); annual mean, areas F4–E4	1958 – 2004	A. Bode (pers. comm.)
70	COP_m	Copepod abundance (from CPR; no. × 10^3 $(3\ m^3)^{-1}$), areas F4–E4	1958 – 2004	A. Bode (pers. comm.)
71	PZI	Phytoplankton–zooplankton index (from CPR), areas F4–E4	1958 – 2004	A. Bode (pers. comm.)
72	PZI_F4	Phytoplankton–zooplankton index (from CPR), area F4	1958 – 2004	A. Bode (pers. comm.)
73	PZI_E4	Phytoplankton–zooplankton index (from CPR), area E4	1958 – 2004	A. Bode (pers. comm.)

4 Methods

Hugo Mendes and Manuel Vargas-Yáñez

Principal component analysis (PCA) has been used to identify coherent patterns of variability objectively among the available time-series. This reduces the dimensionality of the data matrix to a smaller number of uncorrelated and possibly meaningful time-series (PC scores) and loading vectors (Von Storch and Zwiers, 1999). It is particularly useful when investigating regime shifts, in part because it requires no *a priori* assumptions about candidate regime-shift years (Mantua, 2004). Additionally, time-series analysis methods must be used to assess the statistical significance and character of temporal changes in the PCs. Nevertheless, according to Mantua (2004), there are well known weaknesses in the use of PCA. First, it is a linear method so it cannot identify non-linear relationships between different input variables. Second, the resulting loading vectors and PC score-pairs are orthogonal. Both characteristics may lead to erroneous interpretations in cases where the resulting PC scores and loading vectors fail to reproduce the true characteristics of the input data matrix. Therefore, identifying statistically significant shifts in PC scores requires additional methods of time-series analysis to be applied subsequently.

We inspected different methodologies available to analyse fish catch time-series and their relationship with environmental conditions. Also addressed were the problems of identifying high frequency and low frequency time-scales present in the catch time-series and how they interact and are affected by environmental forcing.

The variability time-scale present in fishery and climate time-series ranges from long-term trends, represented by linear trends, to low-frequency (typically multidecadal) oscillations and high-frequency variability consisting of interannual variability.

The statistical tools described were applied to the regional case study of sardine catches in Portuguese waters, to exemplify the methodology to treat the autocorrelation that reflects the memory of the time-series in the system.

Figure 4.1 shows the catch time-series in northwest Portugal. Initially, we tested for the presence or absence of a long-term linear trend by fitting a straight line using a least-squares fit. The anomalies relative to this linear trend were calculated by subtracting the trend from the mean value, obtaining detrended anomalies with a variability containing both the decadal (low frequency) and interannual (high frequency) drivers.

The autocorrelation of this time-series was then estimated at different time-lags (upper left corner of Figure 4.1). Catches in northwest Portugal are obviously strongly autocorrelated, because the correlations are positive up to a ten-year delay. This simply reflects the strong memory of the system and the influence of each single datapoint on the following one. From a statistical perspective, it implies that consecutive datapoints are not statistically independent and that each datapoint does not provide one more degree of freedom. Statistical significance for the linear trend detection took this into account with a loss of 91 degrees of freedom, down to 18 effective degrees of freedom (e.d.f.). This correction is made using the expression: $\text{e.d.f.} = L/\tau$, where L is the total length of the time-series and τ is the integral time-scale, calculated as

$$\tau = \int_{0}^{\mathrm{ZERO}} \rho(k)\mathrm{d}k\,,$$

where $\rho(k)$ is the correlation coefficient for lag k, and ZERO denotes the first zero crossing of the autocorrelation function. Taking into account the loss of degrees of freedom, the decreasing linear trend was not statistically significant at the 95% confidence level.

The following step is to estimate the low frequency by means of a five-year moving average (the blue line in Figure 4.1), and once it is subtracted from the original series, the high frequency trend is left (red line in Figure 4.1). The same analysis was performed for NAO, northwesterly winds, and SST time-series, and a linear regression of the northwest catches on each of the variables was also determined.

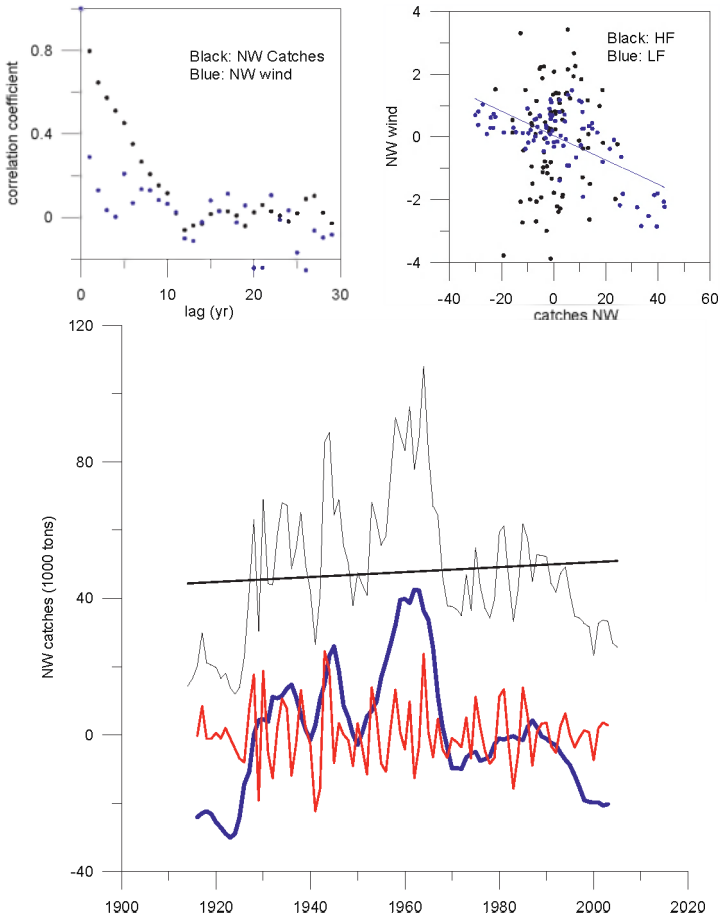

Figure 4.1. Autocorrelation function for northwest Portugal sardine catches and northwest wind (bottom). Adjusted linear trend to the northwest catches (top right).

The regression of the northwest Portuguese anchovy catches on northwesterly winds for the high-frequency time-series revealed that these two variables are not correlated at this short time-scale. The upper panel in Figure 4.2 shows the northwest catches in black, and the reconstructed time-series using the linear model in red for the high-frequency time-series, and the lower panel the same analysis for the low-frequency northwest catches. Again, the black line is the time-series and the red one is the reconstructed series from the regression on the northwest wind. In that case, the explained variance is 47%. Interestingly, the results improve for interannual variability (9% variance explained) when the catches are regressed on the NAO

index, but the results are worse for low frequency. Note, however, that there is a negative relationship between NAO and catches for the decadal variability.

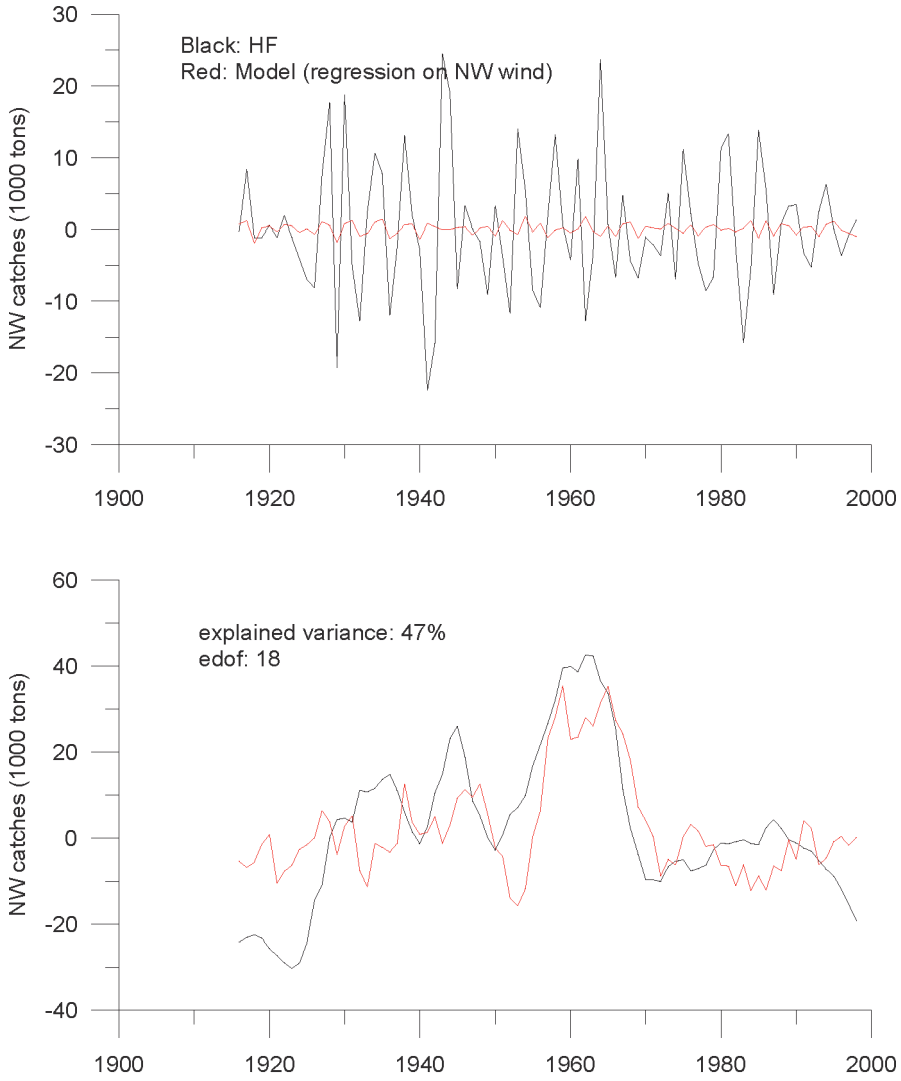

Figure 4.2. Short-term regression (top) and long-term regression (bottom) between northwest Portugal sardine catches and the winter north wind, showing northwest catches (black) and the reconstructed series from the model (red).

Finally, we performed a multiple regression analysis of the northwest catches on the NAO and northwesterly winds and for high- and low-frequency time-series (Figure 4.3). The model was able to explain 11% of the variance for the interannual variability and was positively correlated with NAO and negatively with northwesterlies. For low frequency, the explained variance is 52%. Even considering the lost degrees of freedom (d.f.) for this case (d.f. = 91; e.d.f. = 18), the correlation was significant at the 95% confidence level. The model revealed that catches are influenced negatively by the NAO, contrary to what was observed for high frequency, and also negatively correlated for northwesterly winds.

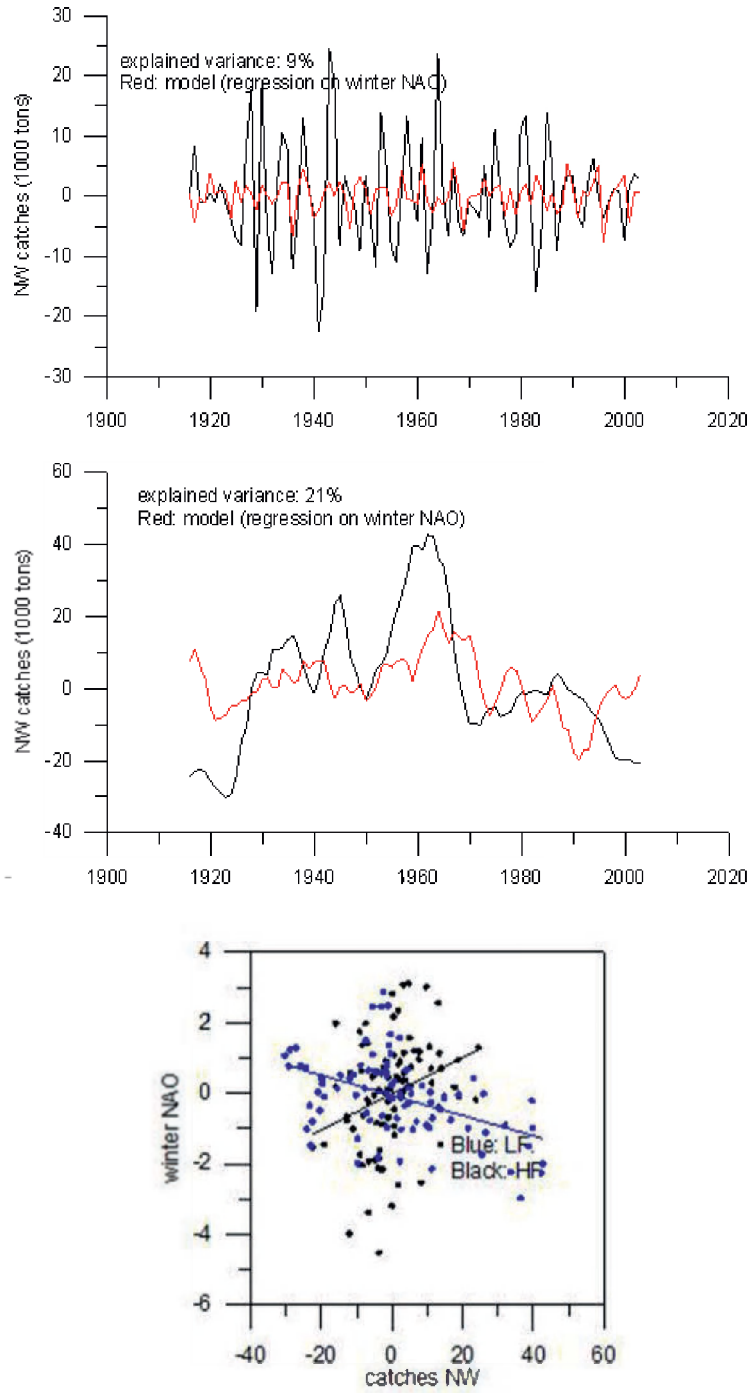

Figure 4.3. Short-term regression (top) and long-term regression model (middle) between northwest Portugal sardine catches and the winter NAO, showing the northwest catches (black) and the reconstructed series from the model (red). The bottom panel shows the line adjusted to the long-term (blue) and short-term series (black).

The approach followed above is based on the time domain. An alternative approach would be to study time-series on the frequency domain, which focuses on investigating periodic properties of the series. To a large extent, the division arises from the type of question being asked of the data. However, combining the approaches can at times give a better understanding of the data. The estimated spectrum decomposes the movement of the series in various sinusoidal waves of different frequency (*f*) and demonstrates the relative strength of each frequency oscillation. The lower frequencies (Figure 4.4 bottom) measure the contribution of

long-term oscillations, and the high frequencies (Figure 4.4. top) measure the contribution of short-term oscillations. Variation in the data at high and low frequencies will correspond to long- and short-term cyclical variation with period = 1/*f*. The shortness of the series–in a time-series perspective–for this case study is one of the limiting factors in analysing periodicity; spectrum analysis made through autoregressive modelling yields better results in short time-series, and that method provides a good estimation of the true spectrum of the series.

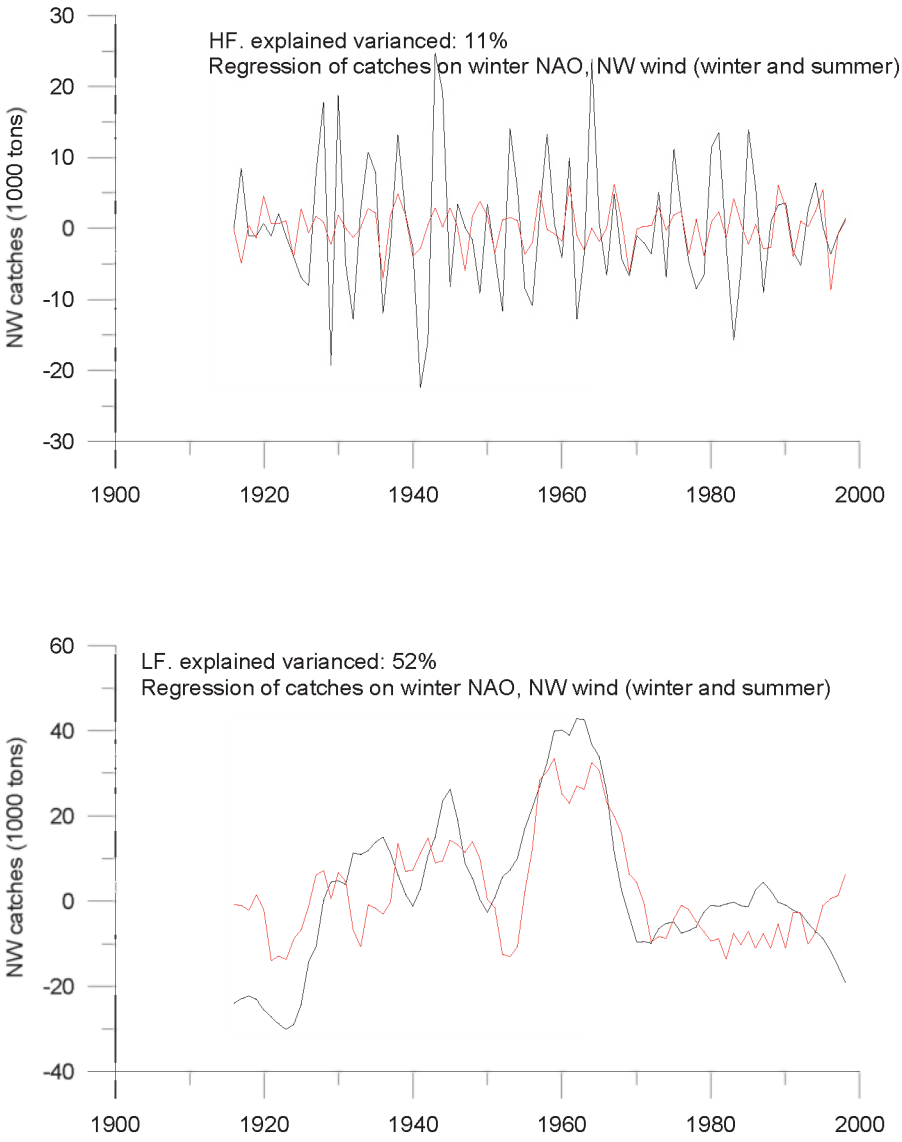

Figure 4.4. Short-term regression (top) and long-term regression model (bottom) between northwest Portugal sardine catches and the predictors winter NAO index and north wind, showing the northwest catches (black) and the reconstructed series from the model (red).

In Figure 4.5, the autoregressive spectral analysis carried out on the northwest, southwest, and western catches is shown. Clearly, the series are dominated by long-term movements with strong memory. There is a common peak in the three regions at a low frequency roughly corresponding to a 20–29 year period. Another low-frequency peak is present in both northwest and southwest catch series, implying a period of ~10 years, corresponding to the memory structure found in the autocorrelation function computed in this study for the northwest area. The remaining high-frequency peaks were dominated by intra-annual variability.

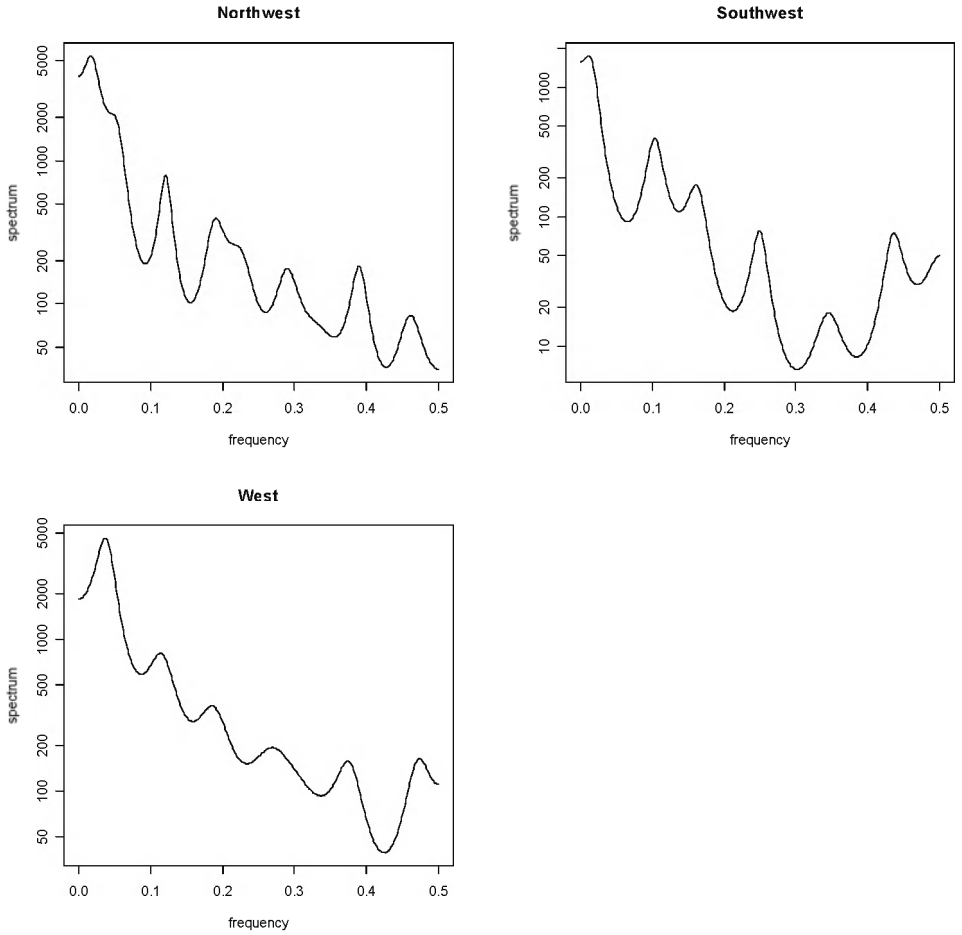

Figure 4.5. Autoregressive spectral analysis for the sardine northwest, southwest, and western catch series.

The statistical time-series analysis was performed using autocorrelation analysis, with the autocorrelation function (ACF) measuring the correlation between observations at different distances apart.

5 Case studies

5.1 Case study 1 – Global region, Atlantic Iberian Peninsula

Antonio Bode, Raquel Somavilla, Alicia Lavín, and Manuel Ruiz-Villarreal

5.1.1 Introduction

The study of variability of climate, oceanographic factors, and key ecosystem components is generally limited by the availability of time-series at long (multi-annual) scales (Bode *et al.*, 2006). Therefore, it was decided to devote notable synthetic effort to the collection and construction of a database including the relevant variables in each of the climate, oceanographic, and ecological subsets, with the database allowing analysis of either regional or subregional patterns. Here, the results of the analysis of the entire Northeast Atlantic near the Iberian Peninsula (Figure 5.1) are presented. For the purpose, variable values obtained at local or subregional levels were integrated or averaged to provide estimates representative of the whole region. Alternatively, only a single variable representing relevant indicators was selected in cases where measurements were available for several sites or subregions.

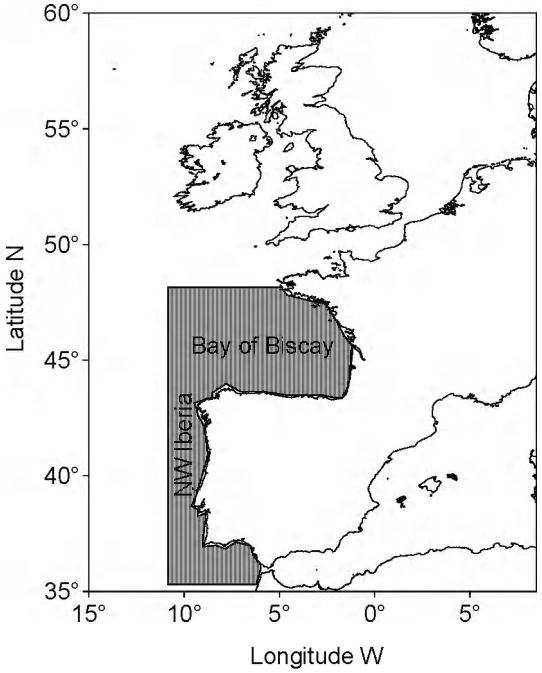

Figure 5.1. Map of the study region (shaded) in the Northeast Atlantic. (ICES, 2007.)

5.1.2 Objectives

The objectives of the case study were to identify and analyse (i) linear trends and (ii) oscillations at a multi-annual scale.

5.1.3 Methods

Variables

Climate variables were provided mainly by teleconnection indices computed for the northern hemisphere (NOAA Climate Prediction Center). The data used in the analysis were annual standardized means from principal component analysis (PCA) of monthly values covering the period 1950–2005. Only four indices were employed

(Table 5.1) as representative of the main drivers of atmospheric circulation over the Northeast Atlantic (Barnston and Livezey, 1987) and taking into account the results of preliminary analysis in the context of the present study (Bode *et al.*, 2006). The North Atlantic Oscillation (NAO), computed as the atmospheric pressure anomaly between Iceland and southern Europe, was associated with dominant climatic conditions over western Europe (Hurrell and Dickson, 2004), whereas the East Atlantic pattern (EA), which is structurally similar to the NAO, contains a strong subtropical component. Scandinavia (SCA) and Polar/Eurasia (POL) patterns are characterized by atmospheric pressure anomalies in boreal regions affecting the longitudinal circulation of winds and storms.

Table 5.1. Variables selected for the regional analysis. The period of data covered, along with the interannual linear trend and significance (p), is also indicated.

VARIABLE	DEFINITION	START–END	TREND	*P*
NAO	North Atlantic Oscillation [1]	1950 – 2005	0.007	0.014
EA	East Atlantic pattern [1]	1950 – 2005	0.016	0.000
SCA	Scandinavia pattern [1]	1950 – 2005	–0.007	0.021
POL	Polar/Eurasia pattern [1]	1950 – 2005	–0.001	0.773
AMO	Atlantic Multidecadal Oscillation [2]	1940 – 2005	–0.001	0.282
Ulm_4311	Mean upwelling index at 43 °N 11 °W [3]	1966 – 2005	–4.798	0.006
TPEA	Mean water transport from the potential energy anomaly, North Atlantic [4]	1955 – 2005	0.104	0.013
SHF_4503	Mean sensible heat fluxes at 45 °N 03 °W [5]	1948 – 2005	0.265	0.000
ZMF_4503	Mean zonal momentum flux at 45 °N 03 °W [6]	1948 – 2005	0.000	0.356
Sardine	Sardine landings [7]	1940 – 2005	–0.601	0.021
Anchovy	Anchovy landings [8]	1943 – 2005	–0.670	0.000
PCI	Phytoplankton colour index [9]	1958 – 2004	0.011	0.000
COP	Copepod abundance [10]	1958 – 2004	–0.008	0.001
ACA	*Acartia* abundance [10]	1958 – 2004	–0.006	0.001
CAL	*Calanus* abundance [10]	1958 – 2004	–0.002	0.047

[1] Teleconnection indices. Annual standardized means of PCA values (relative scale units). ftp://ftp.cpc.ncep.noaa.gov/wd52dg/data/indices/tele_index.nh.

[2] SST anomaly from detrended mean global warming value. http://web1.cdc.noaa.gov/Timeseries/AMO/.

[3] Offshore water transport estimated from geostrophic winds (Lavín *et al.*, 1991). Annual means ($m^3\ s^{-1}\ km^{-1}$).

[4] Annual means ($Mt\ s^{-1}$).

[5] Annual means ($W\ m^{-2}$) computed from values provided by http://www.cdc.noaa.gov/cdc/data.coads.2deg.html.

[6] Annual means ($N\ m^{-2}$) computed from values provided by http://www.cdc.noaa.gov/cdc/data.coads.2deg.html.

[7] Commercial catches in ICES Divisions VIIIc and IXa (ktonnes). http://www.ices.dk.

[8] Commercial catches in ICES Divisions VIIIa,b,c and IXa (ktonnes). http://www.ices.dk.

[9] CPR areas F4 and E4. Annual means (relative scale units). http://www.sahfos.org.

[10] CPR areas F4 and E4. Annual means (no. $\times 10^3$ $sample^{-1}$). http://www.sahfos.org.

The five oceanographic variables retained were representative of vertical stability of the upper water column, SST, and east–west oceanographic gradients (Table 5.1). The Atlantic Multidecadal Oscillation (AMO) was significantly correlated ($p < 0.05$) with all other variables, indicating SST at various sites in the region, with the advantage over individual site values of providing an integrated value for the entire North Atlantic basin (Kerr, 2000). Similarly, sensible (SHF_4503) and zonal (ZMF_4503) heat fluxes were preferred to values of sea temperature or wind because they are related

to water-column stability and turbulence caused by windstress, respectively (Curry and Webster, 1999; Siedler *et al.*, 2001). Heat fluxes were computed from temperature and windspeed values at the sea surface in a 2° × 2° cell centred at 45°N 03°W provided by the International Comprehensive Ocean–Atmosphere Dataset (ICOADS). Transport of water was estimated from the potential energy anomaly (TPEA), a two-point baroclinic pressure difference between the subtropical and subpolar gyre centres derived from hydrographic measurements in the Labrador Basin and at Station S near Bermuda (Curry and McCartney, 2001). This transport index indicates variations in main North Atlantic currents such as the Gulf Stream and the North Atlantic Current.

The role of upwelling was represented by the dataseries of the Ekman transport values computed at a 2° × 2° cell centred at 43°N 11°W (Lavín *et al.*, 1991), because that series was significantly correlated with most other indices of upwelling available for the region ($p < 0.05$). The annual mean of the upwelling index (UIm_4311) was selected in this case because of the better correlation of this series with other oceanographic variables, compared with seasonal means, and because the mean value was expected to balance the positive and negative effects of upwelling on pelagic fish (Guisande *et al.*, 2001; Borges *et al.*, 2003). Biological variables included plankton abundance and/or biomass values from the CPR survey (http://www.sahfos.org/). Data were averaged over CPR grids F4 (northwestern Iberian shelf) and E4 (Bay of Biscay) between 1958 and 2004. Phytoplankton biomass was estimated from the phytoplankton colour index (PCI), and zooplankton abundance was represented by total copepod abundance (COP). To investigate changes in the plankton community that may be relevant to upper trophic levels, the abundance of small copepods, represented by the genus *Acartia* (ACA), and large copepods, represented by the genus *Calanus* (CAL), was also analysed. Planktivorous fish biomass was estimated from the time-series of commercial landings of sardine and anchovy in ICES Subarea VIII (Division VIIIc for sardine) and Division IXa (ICES, 2005).

Statistical methods

A preliminary treatment was to complete the missing data in some variables to ensure continuity of the series in the study period. Data were estimated from significant regression functions with related variables (as for CPR data from nearby zones) or autoregression within the series. In all cases, the estimated data were < 10% of the total in the series. Significance in linear trends in all variables was investigated to reveal interannual rates of change. Thereafter, the trends were removed, and the variables were normalized and standardized for subsequent analysis of multi-annual periods. The main patterns of interannual variability in climate and oceanography were summarized through PCA of the selected variables. These analyses were repeated with different combinations of variables to identify the components demonstrating the best correlations with all other variables (including those not used in the PCA). For biological variables, the analysis of multi-annual periods was performed with the original variables and also with several ecosystem indices, the latter aimed at revealing changes in ecosystem structure. These indices were computed as differences of the detrended, normalized, and standardized values of paired variables, such as the phytoplankton–zooplankton index (PZI = PCI–COP), the *Acartia–Calanus* index (ACI = ACA–CAL), and the relative indicator series (RIS = sardine–anchovy). The computation procedure and rationale are based on those described by Lluch-Cota *et al.* (1997) for the study of alternating species of pelagic fish.

Finally, the relationships between interannual changes in the relevant indices were analysed in order to explore the instantaneous link between climate, oceanographic, and ecosystem variables. The latter are referred to as components of short lifespan, such as plankton and planktivorous fish that are able to respond immediately to changes in environmental conditions.

5.1.4 Results

Climate

All indices selected, except POL, demonstrate significant linear trends during the period analysed (Table 5.1). NAO and, particularly, EA increased, whereas SCA decreased between 1950 and 2005. These indices can be considered as independent because they were uncorrelated one to another (p >0.05). The first two principal components retain 59% of the total variance (Table 5.2), with the first component (32%) representing the effect of northern vs. subtropical modes (NAO and EA), whereas the second component (27%) indicates the variability of boreal modes (SCA and POL). Positive anomalies of CLI1 were observed in the periods 1964–1978 and 1989–1997, whereas negative anomalies dominated in the periods 1950–1963, 1979–1989, and 1998–2005 (Figure 5.2). The duration of each phase is ca. 15 years before 1978, and 9 years thereafter. Such variations correspond mostly with EA, particularly after the 1960s. Variability in CLI2 is characterized by alternating positive and negative anomalies every 3–10 years, mirroring the variations in SCA after the 1960s (Figure 5.2).

Table 5.2. Correlations between the original variables and the first (CLI1) and second (CLI2) components of the PCA on climate variables.

Variable	PC1	PC2
NAO	0.586	0.162
EA	-0.689	0.155
SCA	0.449	-0.759
POL	0.532	0.663

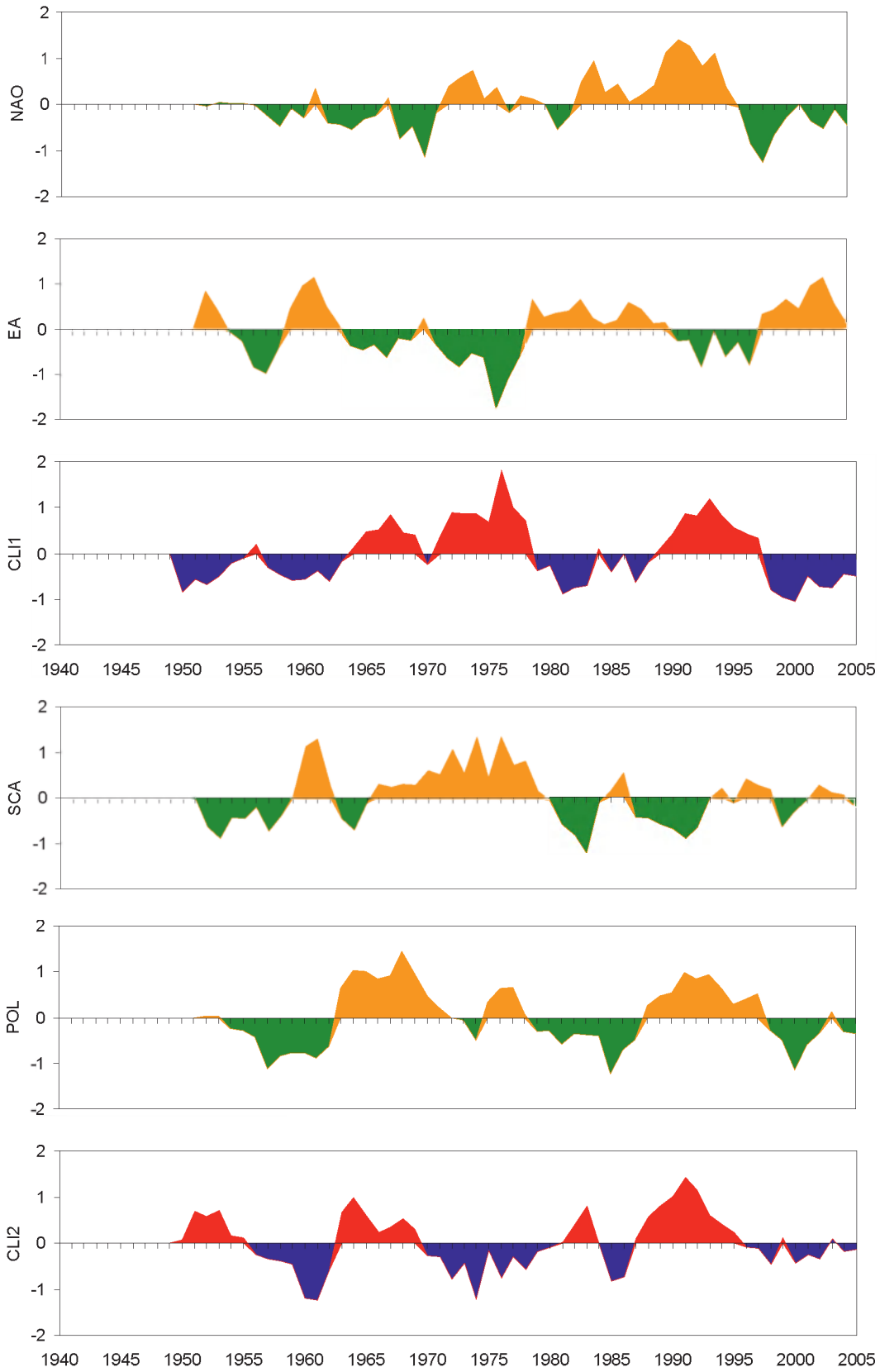

Figure 5.2. Anomalies of climate variables with the long-term trend removed, contributing to the first (CLI1) and second (CLI2) components extracted by a PCA. NAO = North Atlantic Oscillation; EA = Eastern Atlantic pattern; SCA = Scandinavia pattern; POL = Polar/Eurasia pattern. All series have been normalized, standardized, and smoothed with a 3-year running mean. (ICES, 2007.)

Oceanography

No significant linear trends with time were found for AMO and ZMF, whereas SHF and TPEA increase, and UIm_4311 decrease (Table 5.1). These results indicate no increase in the stratification of surface waters as a consequence of the reduction in upwelling in the eastern Atlantic, along with an intensification of water transport by the North Atlantic gyre. The PCA analysis performed on these variables, after excluding UIm_4311 because of the lack of values before 1966 and the significant correlation with AMO and ZMF_4503 ($r = -0.330$ and 0.418, respectively, $p < 0.05$), produced two main components accounting for 63% of the total variance (Table 5.3). The first component (OCE1) is related mainly to the variability in SHF_4503 and AMO, as opposed to that in ZMF_4503. This component accounts for 37% of the total variance and can be interpreted as an index of stability in the upper water column of the region, with positive values associated with positive anomalies of AMO and SHF_4503 (i.e. high SST and heat flux from the sea to the atmosphere), and negative values associated with positive anomalies of windstress-causing turbulence. The second component (OCE2) accounts for 26% of the variance and mainly reflects the intensity of water transport by the North Atlantic gyre, as indicated by the high positive correlation with TPEA (Table 5.3). This component is also positively related to turbulence.

Table 5.3. Correlations between the original variables and the first (OCE1) and second (OCE2) components of the PCA on oceanographic variables.

Variable	OCE1	OCE2
AMO	0.614	-0.183
TPEA	0.444	0.788
SHF_4503	0.792	0.107
ZMF_4503	-0.523	0.617

Positive and negative anomalies of OCE1 alternate at a remarkably constant period of twelve years (Figure 5.3). However, a discontinuity is apparent after 1978, when the positive anomaly was extremely short and weak, producing two consecutive negative anomalies separated by just two years. This apparent shift is related to the long period of negative AMO between 1964 and 1995, in which period ZMF_4503 showed a maximum value of negative anomaly in the late 1970s, suggesting a relaxation in the coupling of windstress turbulence and SST. The shift can be also recognized in OCE2, because the oscillations in this component are nearly identical with those of TPEA in recent years (Figure 5.3), but the pattern differed before 1978, when positive anomalies were of short duration (3–4 years).

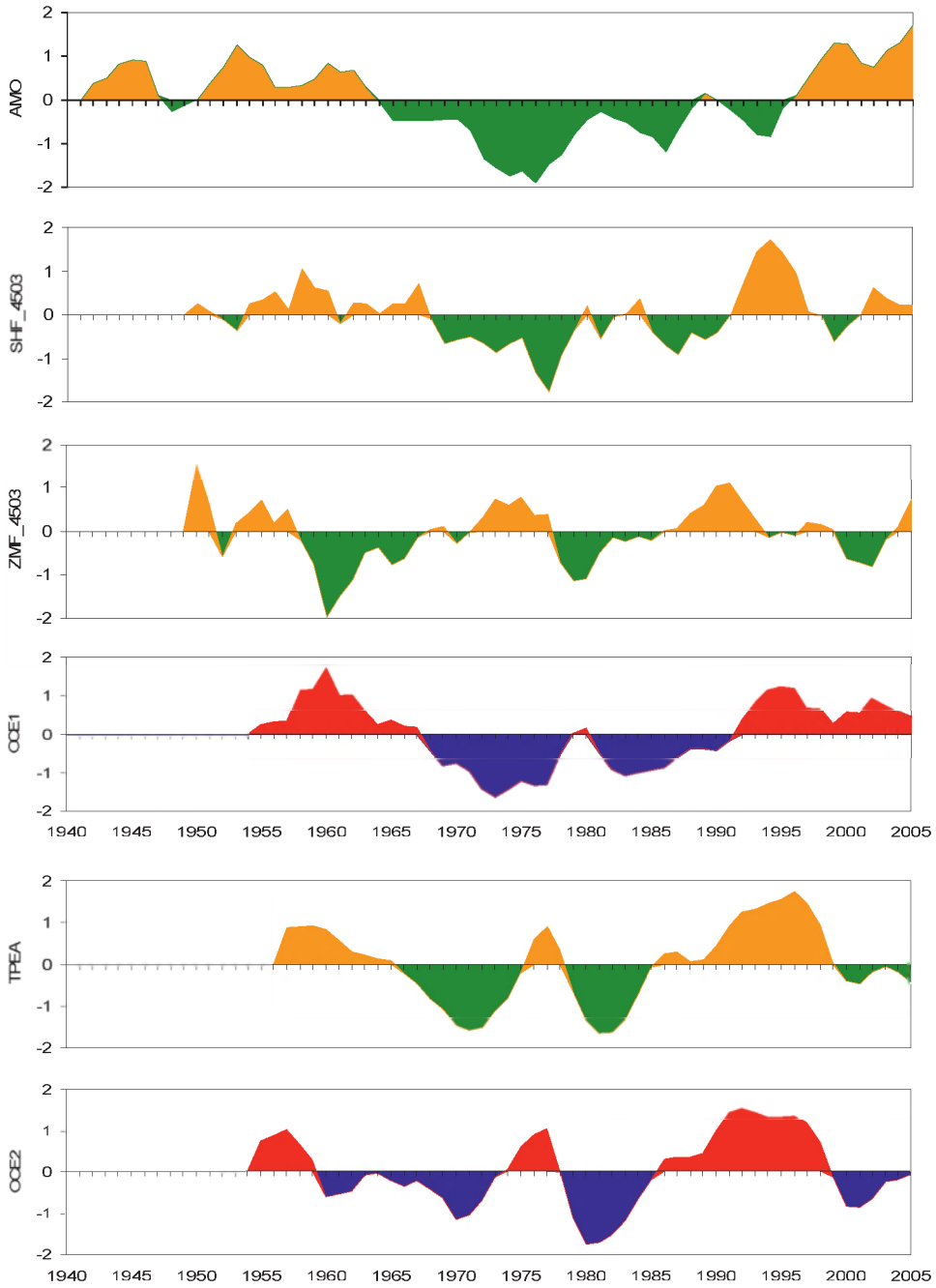

Figure 5.3. Anomalies of oceanographic variables with the long-term trend removed, contributing to the first (OCE1) and second (OCE2) components extracted by a PCA. AMO = Atlantic Multidecadal Oscillation; SHF_5403 = sensible heat flux at 45°N 3°W; ZMF_4503 = zonal momentum flux at 45°N 3°W; TPEA = transport caused by the potential energy anomaly over the North Atlantic. All series have been normalized, standardized, and smoothed with a 3-year running mean. (ICES, 2007.)

Ecosystem structure

Most biological variables display negative trends during the study period (Table 5.1); only phytoplankton biomass (PCI) exhibits a mean increase, whereas copepod abundance and fish biomass decrease for all species considered. Plankton variables are characterized by the succession of relatively short periods (generally < 5 years) of positive and negative anomalies, but paired variables (e.g. PCI vs. COP or *Acartia* vs.

Calanus) do not exhibit consistent match–mismatch patterns (Figure 5.4). The combined indices, however, have relatively longer periods of ca. ten years, particularly after the late 1970s. In this way, an increase in the relative dominance of phytoplankton over zooplankton in recent years can be traced by the longer and higher positive PZI anomalies compared with those observed before 1970 (Figure 5.4). Similarly, there is a decrease in the relative dominance of small over large copepods, indicated by a reduction in the peaks of both positive and negative anomalies of ACI since 1980 (Figure 5.4).

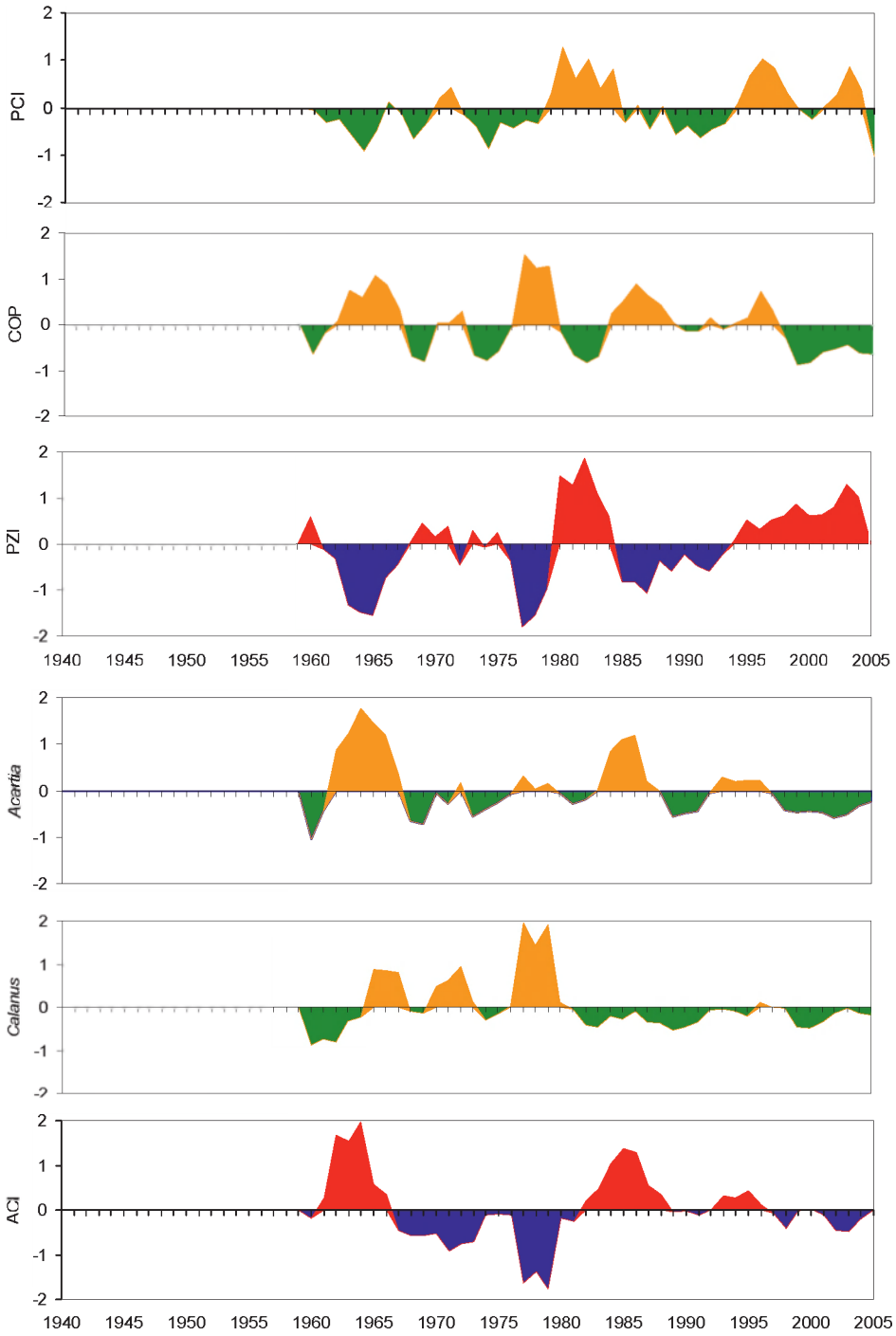

Figure 5.4. Anomalies of biological variables with the long-term trend removed, contributing to ecosystem indices of plankton structure (PZI), zooplankton composition (ACI), and planktivorous fish dominance (RIS). PCI = phytoplankton colour index; COP = copepod abundance; *Acartia* = abundance of *Acartia* spp; *Calanus* = abundance of *Calanus* spp. All series have been normalized, standardized, and smoothed with a 3-year running mean. (ICES, 2007.)

The series of pelagic fish indicates the succession of positive and negative anomaly periods of ca. ten years for both sardine and anchovy (Figure 5.5). Interestingly, the anomalies are in phase before 1980, when both species increase or decrease simultaneously, but out of phase thereafter. This shift in the succession pattern is

reflected by RIS anomalies before the late 1970s, with longer periods and lower amplitude than those observed in recent years. The time of shift can be dated around 1978, when a short period of negative RIS anomaly indicates the start of the mismatch between sardine and anchovy landings.

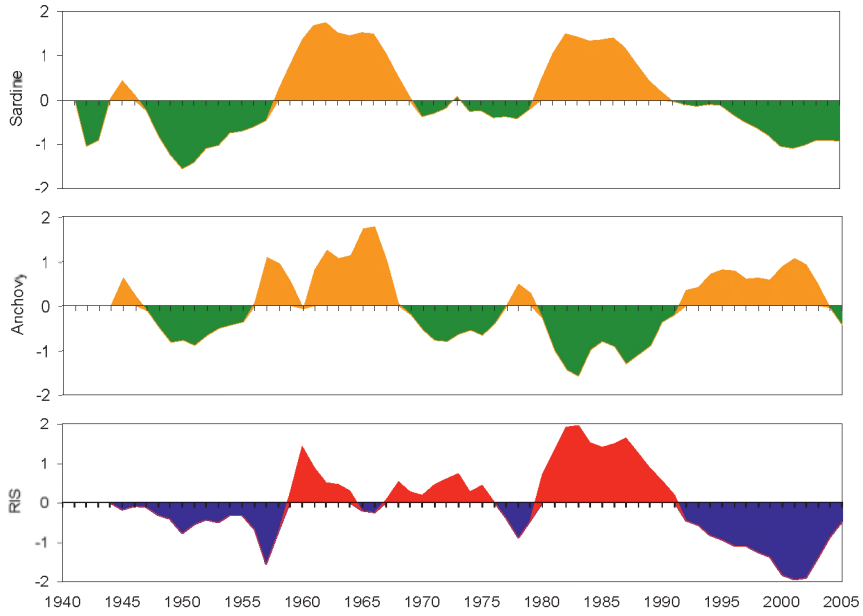

Figure 5.5. Anomalies of sardine and anchovy landings with the long-term trend removed contributing to the regime indicator series index (RIS). All series have been normalized, standardized, and smoothed with a 3-year running mean. (ICES, 2007.)

Comparative analysis

The combination of source variables produce integrated indices with less high-frequency variability than the original, revealing notable time-scale patterns (Figure 5.6). Interannual variability in climate, ocean, and ecosystem properties in the northwest Iberian region, summarized using the principal components and indices computed, is characterized mainly by oscillations at decadal time-scales. A recurrent feature, however, is the shift in correspondence between positive and negative anomalies when comparing different indices. As noted with individual variables, after the late 1970s, anomalies of paired indices changed from in-phase to out-of-phase, or vice versa. For instance, CLI1 and OCE1 anomalies before 1980 are out of phase, but those for the period 1980–1995 are in phase. The positive PZI anomaly period since 1990 is related to positive anomalies of OCE1 and negative anomalies of CLI1, whereas in other periods (as in the late 1960s and 1970s), the converse association applied. More consistent, however, is the association between positive anomalies in ACI and those in RIS, suggesting a major role of trophic factors linking greater abundance of small copepods to the abundance of sardine, and conversely a relative dominance of large copepods to anchovy abundance.

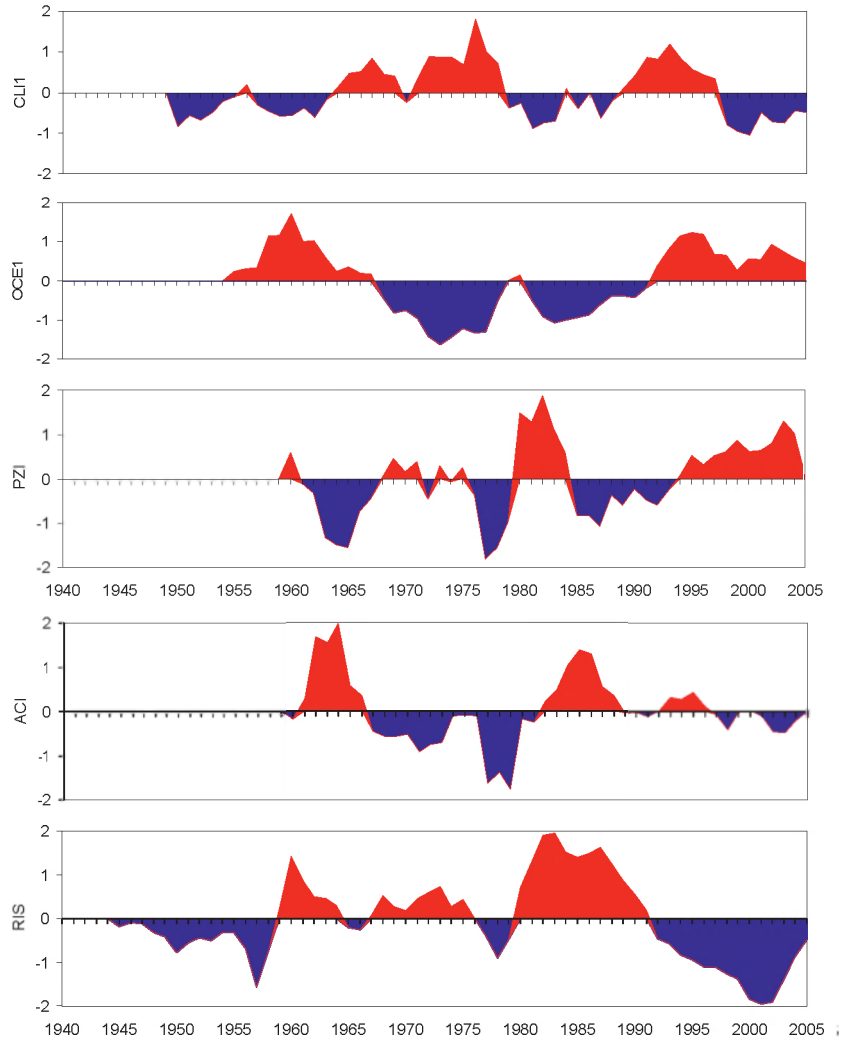

Figure 5.6. Comparison of anomalies of the main climatic (CLI1), oceanographic (OCE1), and ecosystem indices (PZI, ACI, and RIS) obtained in Figures 5.2, 5.3, 5.4, and 5.5. (ICES, 2007.)

Because of the shift in the correspondence of anomalies, the average functional relationships between indices for the whole study period are poor. However, selected linear relationships suggested possible links between climate and ocean factors affecting ecosystem structure (Figure 5.7). Oceanographic variability, as summarized by OCE1, is negatively correlated with the main climate component (CLI1). This is consistent with an increase in ocean turbulence (and upwelling), with the increase in north winds and boreal influence produced in phases of positive NAO, as opposed to an increase in water column stability and higher SST (and a decrease in upwelling) produced in phases of subtropical influence. The decrease in the intensity of the North Atlantic gyre, indicated by OCE2, is associated with a relative increase in phytoplankton in the region (PZI) that may be linked to an enhancement of the effects of upwelling through a reduction in the dispersal of phytoplankton cells into the ocean (Figure 5.7). Finally, RIS is negatively associated with OCE1, particularly if the data for 1958 and 1960 are excluded (Figure 5.7). This relationship demonstrates the positive effect of increasing turbulence (strong windstress) on the relative abundance of sardine during the study, whereas a more stable water column (high mean SST) favours the relative dominance of anchovy. The outliers, which are excluded, are in the period when both species coexisted at high abundance.

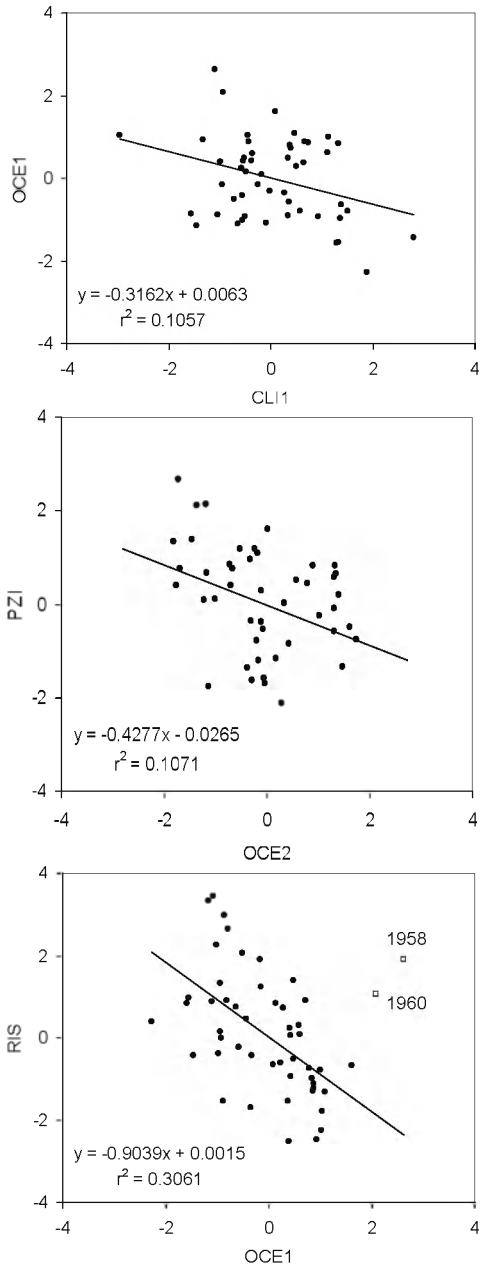

Figure 5.7. Selected examples of linear relationships between the main indices of variability of climate vs. ocean (a), ocean vs. plankton (b), and fish vs. ocean (c). (ICES, 2007.)

5.1.5 Summary and conclusions

Significant interannual trends in climate, oceanographic, and ecosystem variables integrated in the northwest Iberian and Bay of Biscay region indicate clear signs of global warming in the region since ca. 1950.

The regional decrease in copepods and planktivorous fish can be related to reduced upwelling and increased stratification. In contrast, an increase in phytoplankton may be the result of various mechanisms, such as a reduction in turbulence, a lack of coupling between phytoplankton and zooplankton, and an increase in westerly currents in the North Atlantic.

In addition to the interannual trends, multi-annual periods of relative positive and negative anomalies have been identified for all variable types. Quasi-decadal scales

are characteristic of climate, oceanographic, and fish abundance indices, whereas plankton indices display generally shorter periods.

A major shift affecting the succession patterns of positive and negative anomalies of all indices in the late 1970s has been identified. The main changes were related to the periodicity and amplitude of the anomaly oscillations and to the phasing of paired indices.

The mechanisms linking climate to oceanographic and ecosystem variability can be summarized by a conceptual model leading to two alternative states. When boreal components dominate the atmospheric climate over the North Atlantic, active upwelling and a relatively turbulent ocean surface favour the growth of small copepods that are consumed efficiently by filter-feeding sardine. When the climate is influenced by subtropical modes, reduced upwelling and stratification in the upper ocean causes a general reduction in plankton productivity and small copepods. In this situation, anchovy populations can burgeon if large copepods are available.

5.2 Case study 2 – local region, Portugal

Maria de Fátima Borges and Hugo Mendes

The dataset analysed for this region consists of catch time-series from northwestern, western, southwestern, and southern Portugal. Figure 5.8 shows the trend in these catches. By simple visual inspection, some of the main features of the series become obvious. Southern regions off Portugal follow a similar trend, with bigger catches at the start of the century, followed by a decreasing trend until the catches stabilize. The northwestern coast, the region where catches are highest, exhibits an upward trend until the 1970s, after which the series seems to suffer a structural change to a lower mean and variance. One of the main patterns influencing atmospheric and oceanic circulation in the North Atlantic is the NAO. It influences ecosystems in Portuguese waters mainly by leading to northwesterly (upwelling-favourable) winds and a transfer of turbulent kinetic energy to the sea, and by affecting the circulation in the North Atlantic, for instance in the position of the Gulf Stream.

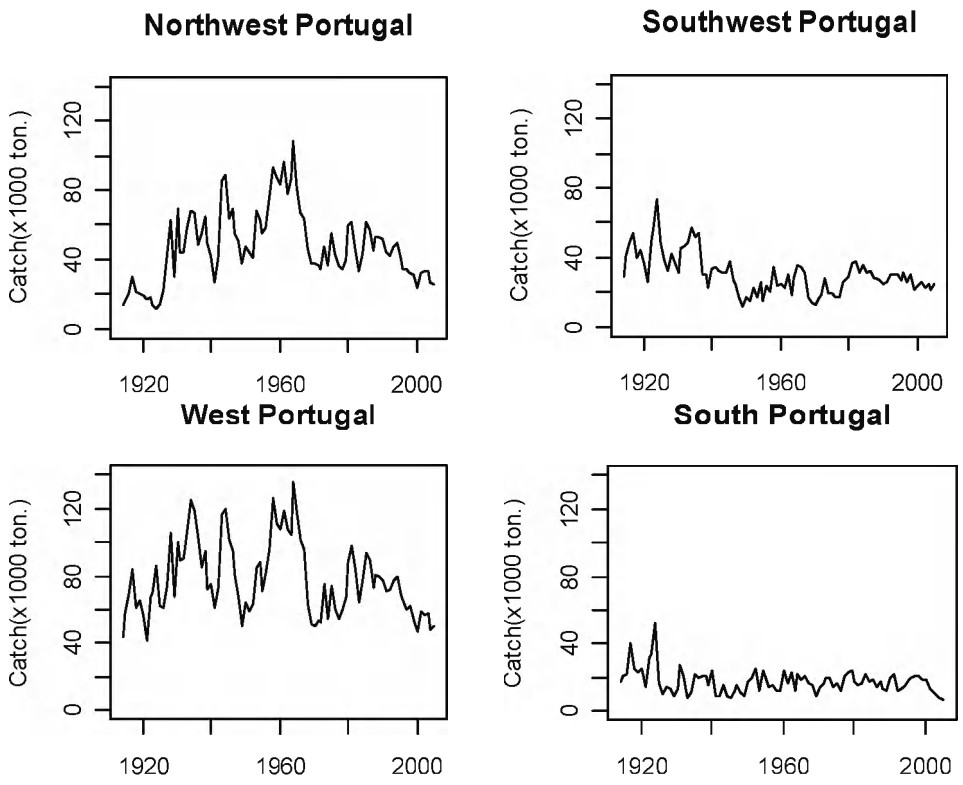

Figure 5.8. Sardine catches from 1915 to 2005 off the northwestern, southwestern, western (combined catches from southwestern and northwestern), and southern regions of Portugal.

Figure 5.9 shows the NAO index and northwesterly wind during the period analysed here, with both variables strongly and positively correlated (northerly winds are considered positive when blowing from the north). Low NAO values during periods of several years seem to correspond to high catches, and vice versa.

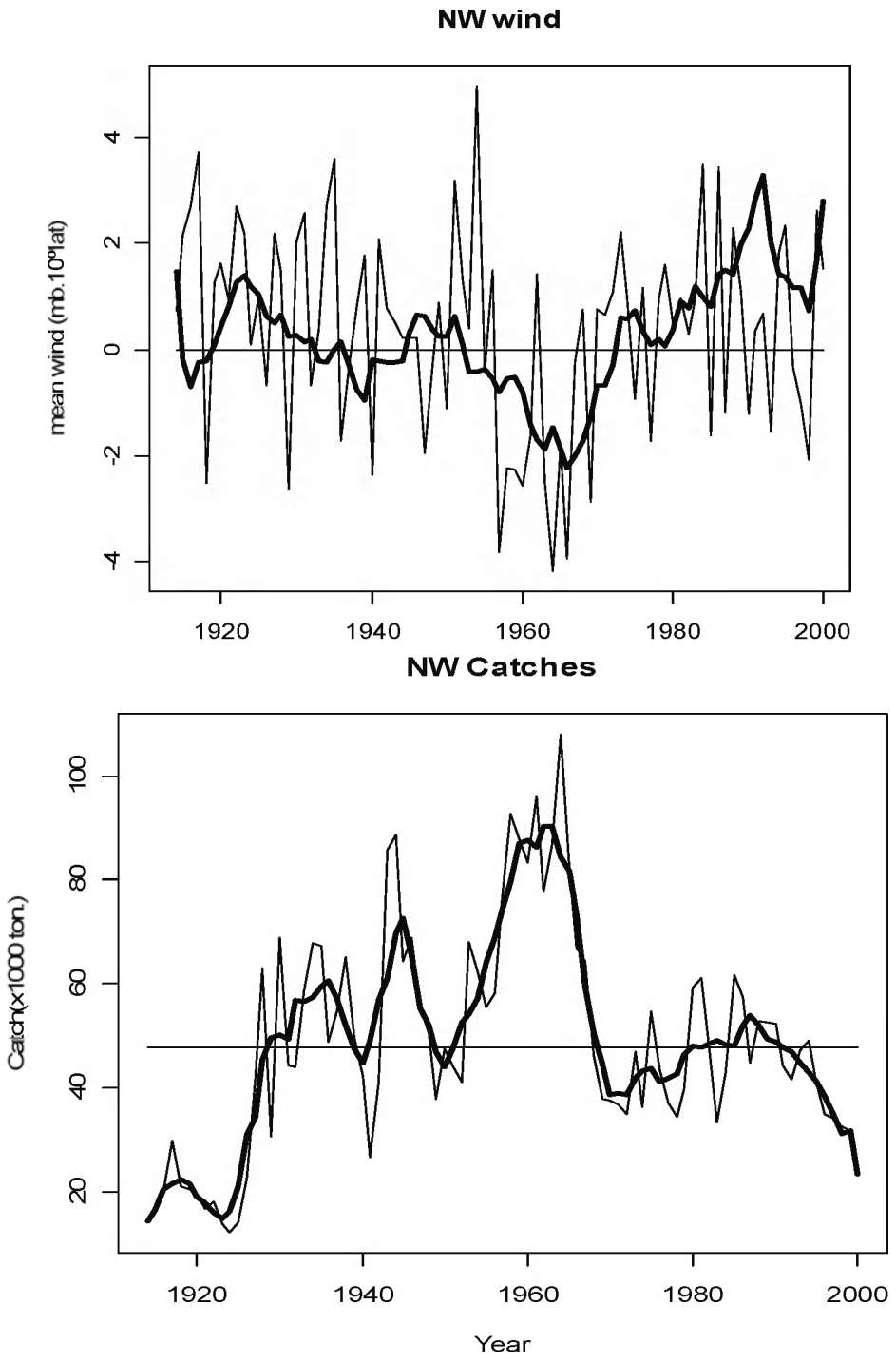

Figure 5.9. Winter NAO index, mean north wind (NW wind), and catches off northwestern Portugal (NW catches); the bold line represents a 5-year moving average.

Visual inspection of the plots reveals low-frequency variability, with alternating increasing and decreasing periods. Although spectral analysis detects it (see following section), these changes seem to have a decadal character. Superimposed on this smooth variability, there is high-frequency variability linked to year-on-year changes in the catches. Figure 5.9 shows the low-frequency variability estimated by means of a 5-year moving average.

Table 5.4. Correlation matrix of the estimated linear association between Portugal's northwestern, southwestern, and southern sardine catches during the period 1914–2005.

	NORTHWESTERN	SOUTHWESTERN	SOUTHERN
Northwestern	1.00		
Southwestern	-0.20	1.00	
Southern	-0.25[1]	0.48[2]	1.00

[1] Significant correlation ($p < 0.05$; 5% level).

[2] Highly significant correlation ($p < 0.001$; 0.1% level).

From the simple linear association, we find a negative correlation between the southern and the northwestern series and a positive highly significant correlation with southwestern catches (Table 5.4).

5.2.1 Time-domain methods

There are two general approaches to analysing time-series. One is to use time-domain methods in which the values of the processes are used directly (autocorrelations). The statistical time-series analysis was performed using autocorrelation analysis. The ACF measures the correlation between observations at different time-lags. Figure 5.10 plots the sample ACF for the four subareas; the two horizontal lines show significance limits at a 95% level. Significant autocorrelation coefficients appear in the northwestern and southwestern regions up to the time-lag of seven and twelve years, respectively. The southern region, despite the significant 1-year-lag correlation, seems to have no clear memory structure.

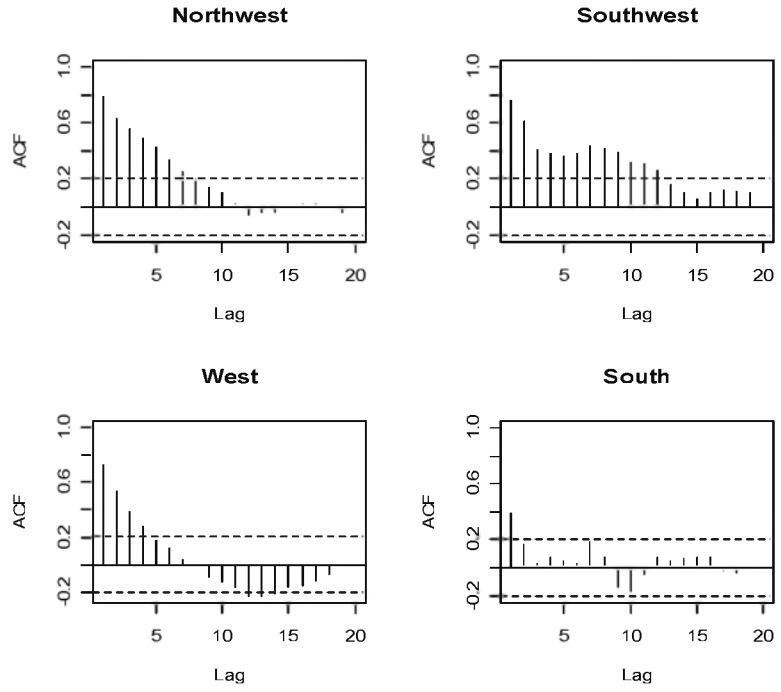

Figure 5.10. Sample autocorrelation function for the areas studied.

Through the sample autocorrelation coefficients, we computed the index of dissimilarity, defined as

$$\sqrt{\sum_{t=1}^{n}\left(\rho_{n,t}-\rho_{m,t}\right)^2}$$

between the different regions up to a 20-year time-lag (Table 5.5).

Table 5.5. Measure of dissimilarity for a 20-year time-lag between the series. The higher the values, the more different are the series in a time-series perspective.

	NORTHWESTERN	SOUTHWESTERN	SOUTHERN
Northwestern	0.00		
Southwestern	0.53	0.00	
Southern	1.28	1.70	0.00

Despite the non-significant linear association between the southwestern and northwestern series, there is similarity in the stochastic pattern. The southern region exhibits no memory structure and clearly distinguishes itself from the other two regions.

5.2.2 Frequency-domain methods

As mentioned above, there are two general approaches to studying time-series; one is the time-domain method; the other is to use frequency-domain methods to investigate the periodic properties of series. Some authors tend to focus on one or the other domain. To a large extent, such division arises from the types of question being asked of the data. However, combining the approaches can, at times, yield a more thorough understanding of the data.

The estimated spectrum decomposes the movement of the series into various sinusoidal waves of different frequency and reveals the relative strength of each frequency oscillation. The lower frequencies (Figure 5.11) measure the contribution of long-term oscillations, and the high frequencies measure the contribution of short-term oscillations. Variation in the data at high and low frequencies will correspond to long- and short-term cyclical variation, with period = $1/f$.

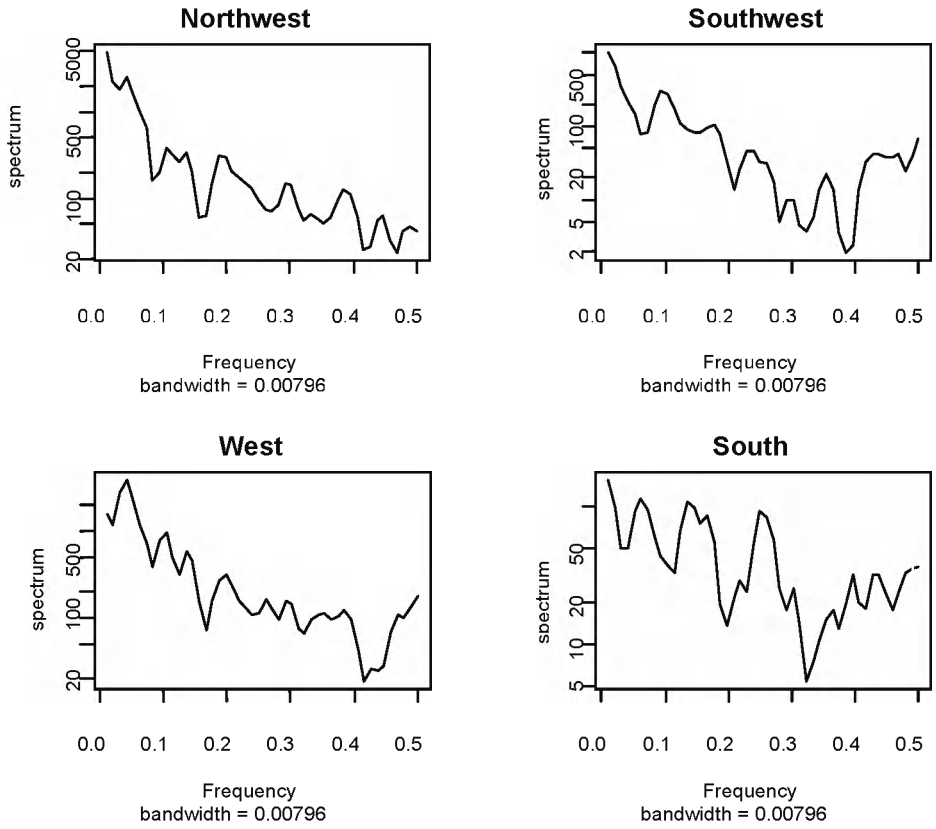

Figure 5.11. Spectrum analysis for northwestern, southwestern, western, and southern Portugal sardine catches.

The shortness of the series in a time-series perspective for this case study is one of the limiting factors in analysing periodicity. Spectrum analysis made through autoregressive modelling yields better results in short time-series, and this method provides a good estimate of the true spectrum of the series. The order was selected here subjectively, based on the partial and autocorrelation function.

The autoregressive spectral analysis made on northwestern, southwestern, western, and southern catches is shown in Figure 5.12. Comparing the result with the standard spectrum analysis, the spectrums of the series in the two methodologies are similar, but the peaks in the autoregressive method seem to be more pronounced.

It is clear that the series are dominated by long-term variance with strong memory. There is a common peak in the three regions at low frequency, roughly corresponding to a period of 20–29 years. Another low-frequency peak is present in both northwestern and southwestern catch series, implying a period of ~10 years. The remaining high-frequency peaks are dominated by intra-annual variability.

From a preliminary analysis made through the cumulative periodogram, a time-series tool that checks whether a series follows white noise (i.e. is a purely random series), it became clear that the peaks in the southern series were not significant.

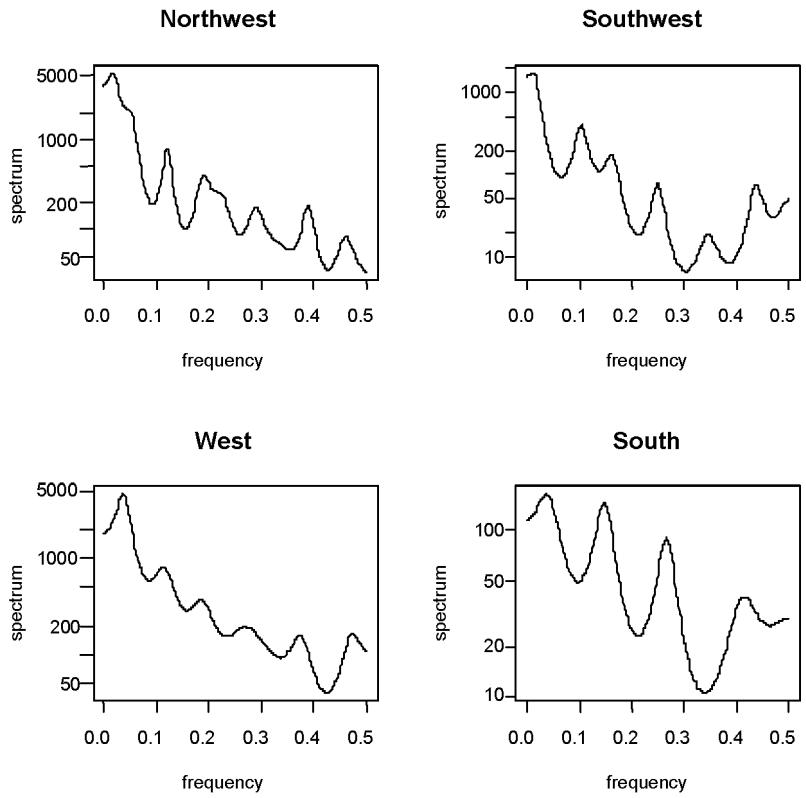

Figure 5.12. Autoregressive spectrum analysis for northwestern, southwestern, western, and southern Portugal sardine catches.

5.3 Case study 3 – local region, Bay of Biscay

Andrés Uriarte and Victor Valencia

The climate and oceanographic features of the inner Bay of Biscay follow the main trends and patterns described above for the Iberian Atlantic coast, following the main trends and anomaly patterns described for the intergyre region of the Northeast Atlantic (Valencia *et al.*, 2003). The ENACW is the main water mass in the upper layers of the Bay of Biscay; it occupies almost the whole water column over the continental shelf and slope. However, the upper layers of the water column suffer some modification (at regional and seasonal scales) largely because of the close coupling between meteorological and oceanographic data in the inner Bay of Biscay (Pérez *et al.*, 1995, 2000; Valencia *et al.*, 2003). For instance, there are clear relationships between atmospheric temperature, SST, heat content, and salinity in relation to the precipitation-minus-evaporation balance and the direct influence of river outflows.

In the Bay of Biscay, two types of ENACW can be identified: colder, fresher ENACWP of subpolar origin, and warmer, more-saline ENACWT of subtropical origin (Ríos *et al.*, 1992). The relative occurrence of those water masses in the southeastern Bay of Biscay, as well as the extent of modification of their characteristics, is related to the main seasonal cycle and to specific climate conditions. During autumn and winter, southerly and westerly winds dominate, and a poleward current prevails, with associated mechanisms of convergence, downwelling, and vertical mixing. During spring and summer, southerly and westerly winds are less prevalent, and northerly and northeasterly winds dominate, with associated mechanisms of divergence, upwelling, and stable stratification. These processes also

increase the proportion of relatively colder, less-saline water (ENACWP) into the southeastern Bay of Biscay in summer (Valencia *et al.*, 2004).

The duality between upwelling and downwelling and the relative prevalence of climate and oceanographic conditions related to these systems seems to be an important factor driving Bay of Biscay anchovy recruitment. Two environmental indices studied during the past ten years (Borja *et al.*, 1996, 1998; Allain *et al.*, 2001) have demonstrated that the prevalence of northeasterly winds during spring and early summer causes weak upwelling and favours the onset of good anchovy recruitment in the Bay of Biscay. In addition, strong gales or storms in June/July, inducing turbulence and disruption of stratification, are detrimental to the success of anchovy recruitment (Allain *et al.*, 2001). Therefore, the balance of windstress and direction in the southeastern corner of the Bay of Biscay has implications for trends in the anchovy population size in the Bay of Biscay.

We review here some of the interrelationships between the general climate indices of the Northeast Atlantic analysed above and some local oceanographic and biological indices for the Bay of Biscay in relation also to anchovy recruitment indices. The analysis is restricted to the period 1967 onwards for which a series of anchovy recruitment indices is available. The indices selected, which reflect some of the relevant features within the Bay of Biscay, are the following subset of the original listing in Tables 3.1–3.3.

Variable acronym	Definition
NAO	North Atlantic Oscillation
EA	Eastern Atlantic pattern
SCA	Scandinavia pattern
POL	Polar/Eurasia pattern
NAO_DM	North Atlantic Oscillation, December–March (Hurrell, 1995)
NAO_m	North Atlantic Oscillation, annual mean (Hurrell, 1995)
AMO	Atlantic Multidecadal Oscillation (SST anomaly from detrended mean global warming value)
RFG	Mean annual river flow, Gironde (Garonne+Dordogne, $m^3 s^{-1}$)
SSTSS	Mean SST at San Sebastian Aquarium (°C)
POLE	Poleward index at 43 °N 11 °W from geostrophic winds (Qy, the October–December quarter of the preceding year)
TPEA	Mean water transport from potential energy anomaly, North Atlantic (Mt s^{-1})
SST_4503	Mean SST (45 °N 03 °W, °C)
UILm_4502	Upwelling index, Landes (45 °N 02 °W, annual mean; $m^3 s^{-1} km^{-1}$)
UIBm_4502	Upwelling index, Basque coast (45 °N 02 °W, annual mean; $m^3 s^{-1} km^{-1}$)
UIBs_4502	Upwelling index, Basque coast (45 °N 02 °W, annual mean of positive values, March–July; $m^3 s^{-1} km^{-1}$)
TURB_4502	Mean annual turbulence, Bay of Biscay (at 45 °N 02 °W; $m^3 s^{-3}$)
SHF_4503	Annual mean sensible heat fluxes, Bay of Biscay (45 °N 03 °W; W m^{-2})
ZMF_4503	Annual mean zonal momentum flux, Bay of Biscay (45 °N 03 °W; N m^{-2})
ARI	Anchovy recruitment index (ICES Subarea VIII; relative units)
AR	Anchovy recruitment (Bay of Biscay, ICES Subarea VIII; no. × 10^9)
HMR	Horse mackerel recruitment (European Atlantic, ICES; no. × 10^9)
PCI_E4	Phytoplankton colour index (from CPR in area E4, Bay of Biscay), annual mean
COP_E4	Copepod abundance (from CPR in area E4; no. × 10^3 $(3\ m^3)^{-1}$)
DWCPR	Mesozooplankton biomass, estimated from abundance for E4+F4 CPR areas (mg DW m^{-3})
PCI_m	Phytoplankton colour index (from CPR in areas F4–E4), annual mean
COP_m	Copepod abundance (from CPR in areas F4–E4; no. × 10^3 $(3\ m^3)^{-1}$)
PZI	Phytoplankton–zooplankton index (from CPR in areas F4–E4)
PZI_E4	Phytoplankton–zooplankton index (from CPR in area E4)

The series were standardized, and any time-trend during the series 1967–2004 was removed. For the Bay of Biscay, a correlation analysis between the above-described variables was performed. Tables 5.6 and 5.7 present the results for selected variables.

This region seems not to be conditioned heavily by the NAO directly. In fact, NAO indices were not related to the hydrographic factors included in the analysis. Only the Gironde River outflow (RFG) was close to being significantly related to the NAO computed from December to March each winter. The East Atlantic pattern (EA), structurally similar to the NAO and Polar/Eurasia (POL) patterns, which affect the longitudinal circulation of winds and storms and are both weakly related to the potential energy anomaly (TPEA), are all related to the upwelling indices of the region (although only occasionally being statistically significant, e.g. POL and TPEA with the spring upwelling index UIBs at 45°02′N).

Both the EA and POL patterns are related significantly to the long recruitment index series of anchovy (ARI), although they do not achieve significance for the short series (AR). This relationship might be related in part to their relationship with the Landes and spring upwelling indices in the region. Gironde River discharge seems to be affected only weakly by the SCA or POL and more directly by NAO from December to March (NAO_DM), the annual upwelling index along Landes (UILm), and with temperature (SSTSS) and sensible heat fluxes (SHF) related to water column stability. Neither temperature nor river discharge are related significantly to anchovy recruitment, although there might be some negative limiting role of river run-off, as indicated by Buffaz and Planque (2006) by quartile regression.

Recruitment of anchovy is significantly influenced by the upwelling index at 45°02′N for both the long (ARI; Borja *et al.*, 1996) and short (AR; ICES, 2005) series, independently or not of retrieving tendencies from the series (Table 5.7). The significance of this environmental index still remains ten years after its first publication in Borja *et al.* (1996). Biological variables from the CPR survey do not demonstrate a clear relationship with anchovy recruitment, except perhaps for the negative relationship demonstrated for mesozooplankton biomass (mg DW m^{-3}) that is estimated from abundance for E4+F4 CPR areas (DWCPR) and not easily understood. However, the positive relationship between the horse mackerel series of recruitment and the phytoplankton–zooplankton index (PZI; CPR areas F4–E4) is interesting, probably resulting from the opposite signs of the potential influences of the copepod and phytoplankton indices on horse mackerel recruitment.

Table 5.6. Selected relationships between climate variables and some oceanographic indices for the Bay of Biscay. Highlighted values indicate a statistically significant relationship. The abbreviations used are defined in the listing preceding this table. (*n* = number of observations.)

DETRENDED	RFG	SSTSS	POLE	TPEA	SST_4503	UILM_4502	UIBM_4502	UIBS_4502	TURB_4502	SHF_4503	ZMF_4503	ARI	AR
NAO	-0.0789	-0.0864	-0.0014	0.0311	-0.0725	0.0704	-0.0491	0.1186	-0.1768	0.1259	0.0932	0.3191	0.0666
n	38	38	38	20	38	36	36	38	36	38	38	37	19
Prob(R)	0.6378	0.6060	0.9934	0.8965	0.6654	0.6832	0.7762	0.4781	0.3022	0.4513	0.5779	0.0543	0.7864
EA	0.1244	0.0169	0.2868	-0.3448	0.0797	-0.2896	-0.1095	-0.2140	0.1013	0.1478	-0.1409	-0.4366	-0.3262
n	38	38	38	20	38	36	36	38	36	38	38	37	19
Prob(R)	0.4567	0.9197	0.0808	0.1366	0.6344	0.0866	0.5250	0.1971	0.5564	0.3758	0.3988	0.0069	0.1729
SOA	0.2699	-0.1933	-0.2828	0.2301	-0.0544	0.0853	-0.0686	-0.0198	0.0656	-0.0933	-0.1317	-0.1158	0.0810
n	38	38	38	20	38	36	36	38	36	38	38	37	19
Prob(R)	0.1013	0.2448	0.0854	0.3291	0.7455	0.6210	0.6910	0.9062	0.7040	0.5773	0.4306	0.4949	0.7417
POL	-0.2362	0.1251	-0.1975	0.3790	0.1315	0.1039	0.1232	0.3305	-0.0138	0.1462	0.1793	0.5030	0.3514
n	38	38	38	20	38	36	36	38	36	38	38	37	19
Prob(R)	0.1533	0.4544	0.2345	0.0993	0.4314	0.5466	0.4740	0.0427	0.9363	0.3811	0.2815	0.0015	0.1402
NAO_DM	-0.3075	-0.1157	-0.0363	0.1271	-0.0514	-0.0261	-0.0341	0.1677	-0.0938	0.1258	0.1669	0.3949	0.1727
n	38	38	38	20	38	36	36	38	36	38	38	37	19
Prob(R)	0.0604	0.4890	0.8289	0.5934	0.7594	0.8797	0.8435	0.3143	0.5865	0.4518	0.3166	0.0156	0.4797
NAOm	-0.1568	-0.0827	-0.0898	0.0343	0.0538	0.1383	-0.1755	0.1237	-0.0593	0.1667	0.1810	0.3460	0.0441
n	36	36	36	20	36	36	36	36	36	36	36	36	19
Prob(R)	0.3610	0.6314	0.6023	0.8857	0.7554	0.4212	0.3059	0.4721	0.7314	0.3311	0.2908	0.0387	0.8578
AMO	-0.0911	0.1999	0.2637	-0.3285	0.2762	-0.1230	-0.0248	-0.1471	0.1953	-0.0835	0.0046	-0.2674	-0.2082
n	38	38	38	20	38	36	36	38	36	38	38	37	19
Prob(R)	0.5864	0.2289	0.1097	0.1573	0.0932	0.4747	0.8856	0.3781	0.2536	0.6181	0.9781	0.1096	0.3923
RFG		-0.3614	-0.0829	0.1864	-0.0984	0.4001	0.1170	0.2887	-0.3222	0.4367	0.0954	-0.2487	-0.0137
n		38	38	20	38	36	36	38	36	38	38	37	19
Prob(R)		0.0258	0.6206	0.4314	0.5568	0.0156	0.4967	0.0788	0.0553	0.0061	0.5688	0.1378	0.9555
SSTSS			0.0736	0.1516	0.4194	-0.3789	-0.2395	-0.4067	0.3767	-0.3637	-0.3282	-0.0198	-0.0325
n			38	20	38	36	36	38	36	38	38	37	19
Prob(R)			0.6607	0.5233	0.0088	0.0227	0.1595	0.0113	0.0236	0.0248	0.0442	0.9072	0.8950
POLE				-0.0066	0.0674	-0.1604	0.0747	-0.0968	-0.0817	-0.0548	-0.0083	-0.2951	-0.1983
n				20	38	36	36	38	36	38	38	37	19
Prob(R)				0.9780	0.6877	0.3501	0.6650	0.5631	0.6359	0.7439	0.9605	0.0762	0.4158
TPEA					0.1416	0.3442	0.2876	0.6343	-0.1109	0.5531	0.0867	0.3114	0.3272
n					20	20	20	20	20	20	20	20	19
Prob(R)					0.5514	0.1373	0.2188	0.0027	0.6415	0.0114	0.7163	0.1814	0.1715

Table 5.7. Selected relationships between oceanographic variables and biological indices for the Bay of Biscay. Highlighted values indicate a statistically significant relationship. The abbreviations used are defined in the listing preceding Table 5.6. (*n* = number of observations.)

DETRENDED	ARI	AR	HMR	PCI_E4	COP_E4	DWCPR	PCI_M	COP_M	PZI	PZI_E4
RFG	-0.2487	-0.0137	0.1960	0.2984	0.1567	0.0134	0.2796	0.2166	0.0492	0.0873
n	37	19	23	38	38	37	38	38	38	38
Prob(R)	0.1378	0.9555	0.3700	0.0688	0.3475	0.9372	0.0891	0.1915	0.7694	0.6021
SSTSS	-0.0198	-0.0325	0.1342	0.1885	-0.1091	-0.0787	-0.0127	-0.1130	0.0781	0.2050
n	37	19	23	38	38	37	38	38	38	38
Prob(R)	0.9072	0.8950	0.5415	0.2571	0.5142	0.6433	0.9399	0.4994	0.6413	0.2171
POLE	-0.2951	-0.1983	-0.1295	0.0442	0.0644	0.0793	0.4289	-0.0299	0.3572	-0.0167
n	37	19	23	38	38	37	38	38	38	38
Prob(R)	0.0762	0.4158	0.5560	0.7922	0.7008	0.6407	0.0072	0.8586	0.0277	0.9206
TPEA	0.3114	0.3272	0.1163	0.5433	0.2527	-0.1362	0.3852	0.4035	0.0474	0.2379
n	20	19	20	20	20	20	20	20	20	20
Prob(R)	0.1814	0.1715	0.6252	0.0133	0.2824	0.5668	0.0935	0.0777	0.8428	0.3124
SST_4503	0.0636	-0.1772	0.2713	0.2408	-0.2520	-0.1830	0.0074	-0.3278	0.2608	0.3429
n	37	19	23	38	38	37	38	38	38	38
Prob(R)	0.7083	0.4681	0.2105	0.1453	0.1269	0.2782	0.9650	0.0445	0.1137	0.0351
UILm_4502	0.4220	0.1790	0.0828	0.0225	-0.0270	-0.0784	0.0580	0.0475	0.0092	0.0341
n	36	19	23	36	36	36	36	36	36	36
Prob(R)	0.0104	0.4634	0.7072	0.8965	0.8759	0.6493	0.7367	0.7834	0.9574	0.8437
UIBm_4502	0.1924	0.1302	-0.1444	-0.0152	0.0779	0.1142	-0.0313	0.1041	-0.1024	-0.0650
n	36	19	23	36	36	36	36	36	36	36
Prob(R)	0.2610	0.5953	0.5108	0.9298	0.6516	0.5072	0.8561	0.5455	0.5523	0.7065
UIBs_4502	0.3973	0.4812	0.2032	0.1265	0.1279	0.0027	0.0232	0.1112	-0.0685	-0.0073
n	37	19	23	38	38	37	38	38	38	38
Prob(R)	0.0149	0.0370	0.3524	0.4492	0.4439	0.9873	0.8899	0.5061	0.6829	0.9654
TURB_4502	-0.1571	0.0877	0.0625	0.1699	-0.0924	-0.1934	0.0703	-0.0619	0.1008	0.1791
n	36	19	23	36	36	36	36	36	36	36
Prob(R)	0.3601	0.7210	0.7768	0.3218	0.5921	0.2585	0.6836	0.7200	0.5585	0.2960
SHF_4503	0.0031	0.0416	0.2983	0.0710	-0.1870	-0.1476	0.1049	-0.0909	0.1524	0.1822
n	37	19	23	38	38	37	38	38	38	38
Prob(R)	0.9854	0.8656	0.1668	0.6718	0.2610	0.3832	0.5308	0.5873	0.3610	0.2736
ZMF_4503	0.2228	-0.1619	-0.1431	-0.0741	-0.0009	0.0451	-0.1222	-0.0388	-0.0649	-0.0491
n	37	19	23	38	38	37	38	38	38	38
Prob(R)	0.1851	0.5079	0.5148	0.6583	0.9957	0.7911	0.4650	0.8170	0.6986	0.7699

Detrended	ARI	AR	HMR	PCI_E4	COP_E4	DWCPR	PCI_M	COP_M	PZI	PZI_E4
ARI		0.8504	0.4024	-0.0366	0.0430	-0.0564	-0.0593	-0.0848	0.0200	-0.0545
n		19	23	37	37	37	37	37	37	37
Prob(R)		0.0000	0.0569	0.8296	0.8007	0.7404	0.7275	0.6178	0.9067	0.7485
AR			-0.1760	0.1480	-0.0316	-0.5540	-0.2664	-0.1331	-0.1496	0.1652
n			19	19	19	19	19	19	19	19
Prob(R)			0.4711	0.5453	0.8977	0.0139	0.2702	0.5871	0.5410	0.4990
HMR				0.4487	-0.2351	-0.1976	0.4975	-0.2556	0.6471	0.4872
n				23	23	23	23	23	23	23
Prob(R)				0.0317	0.2802	0.3661	0.0157	0.2391	0.0008	0.0184

6 General discussion

Antonio Bode, Jürgen Alheit, Alicia Lavín, Andrés Uriarte, and Maria de Fátima Borges

6.1 Trends and global warming

All the observed trends are consistent with a general increase in both atmospheric and sea surface temperature in the late 20th century (Kerr, 2000; Hansen *et al.*, 2005). Considering the study period, the influence of boreal components (e.g. north winds indicated by positive NAO values) on the climate in the North Atlantic declined, whereas that of subtropical components (e.g. EA) increased. This influence may explain the increasing stratification of surface waters, the reduced upwelling in the eastern Atlantic, and the intensification of water transport to the east by the North Atlantic gyre. This interpretation is consistent with observations (Curry *et al.*, 2001) and model predictions of North Atlantic currents (Bryden *et al.*, 2005). The overall decrease in zooplankton and fish is also consistent with an increase in stratification at the surface, which itself would reduce productivity. Similar trends were reported using CPR data over the North Atlantic, revealing a reduction in phytoplankton in warmer regions, whereas that of cooler regions increased (Richardson and Schoeman, 2004). In this way, the increase observed in phytoplankton biomass when upwelling intensity drops may be explained by either metabolic enhancement through the increasing temperature or a progressive uncoupling from zooplankton consumers (Edwards and Richardson, 2004). A similar increase in recent years has been described for coastal phytoplankton at some sites within the study region (Bode *et al.*, 2006). Although there is evidence of strong bottom–up control of climate on the planktonic foodweb, several mechanisms have been invoked to explain the changes (Beaugrand, 2004; Edwards and Richardson, 2004; Richardson and Schoeman, 2004). Because of the rapid response of plankton to oceanographic conditions, comparative studies between adjacent regions may reveal the dominance of a particular mechanism in shaping planktonic communities. For instance, the rate of change of zooplankton communities varies along the northern Iberian coast in relation to the change in water-column stratification (Valdés *et al.*, 2007).

6.2 Periodic changes and bottom-up forcing

The study revealed the succession of periods at interannual, in many cases, quasi-decadal, scales for climate, oceanographic, and ecosystem indices. Similar changes have also been shown for other regions characterized by coastal upwelling (e.g. Chavez *et al.*, 2003). Interestingly, the changes off northwest Iberia were in an upwelling system characterized by a range in variability of absolute values of upwelling intensity and ecosystem productivity much smaller than those in other oceanic regions, such as Peru or South Africa (Schwartzlose *et al.*, 1999). It must be taken into account, however, that the database used only spans up to 60 years, allowing for the identification of only a few decadal periods. Therefore, the role of different mechanisms can only be advanced tentatively. In any case, what can be explored is the possible role of direct effects of climate vs. foodweb-mediated controls on the observed succession of alternative states of the ecosystem.

Direct effects of climate on plankton and sardine populations have been demonstrated in subzones of the study area. For instance, several studies (Dickson *et al.*, 1988; Borges *et al.*, 2003; Guisande *et al.*, 2004) analysed the negative relationship

between the intensity of northerly winds in spring and sardine landings off Portugal and Galicia. Other studies have revealed the negative effect of intensive winter and spring upwelling on the recruitment of sardine, likely by increasing larval dispersion (Guisande *et al.*, 2001; Santos *et al.*, 2004). In contrast, moderate upwelling seems to favour anchovy recruitment in the eastern Bay of Biscay (Borja *et al.*, 1998; Allain *et al.*, 2001). In addition to direct effects of climate and oceanographic conditions, indirect effects on upper trophic levels may operate through changes in productivity and the structure of plankton communities (Chavez *et al.*, 2003; van der Lingen *et al.*, 2006). In the latter case, the availability of appropriate prey favours the dominance of one or other species of planktivorous fish. Adult sardine are better suited than anchovy to filter-feeding on small copepods, but anchovy are efficient predators of large copepods (van der Lingen *et al.*, 2006). In addition, sardine can consume phytoplankton (Bode *et al.*, 2004; Cunha *et al.*, 2005). These trophic characteristics may favour the dominance of one fish species when the environmental conditions for the development of appropriate food are right. For the southern Benguela, intermittent upwelling is hypothesized as the driver of high phytoplankton biomass in large cells that feed large copepods, thus favouring anchovy dominance (van der Lingen *et al.*, 2006). Warm surface waters during reduced upwelling conditions are related to the proliferation of small phytoplankton cells and copepods, which are ideal forage for sardine. Similar hypotheses were proposed for the Pacific (Chavez *et al.*, 2003), although the association between upwelling intensity and a particular fish species seems to vary among geographic locations (Chavez *et al.*, 2003; Bertrand *et al.*, 2004).

The link between climate, oceanography, and the structure of the ecosystem in Iberian waters of the North Atlantic can be formulated as a conceptual model in which alternative modes of the climate system lead to divergent oceanographic conditions and, in turn, to the dominance of alternative plankton and fish species (Figure 6.1). On one side, the dominance of boreal climate modes, such as those indicated by positive NAO, and the influence of northerly winds and pressure anomalies is associated with increased turbulence at the ocean surface, relatively low water temperature, and high average intensity of upwelling. Such conditions favour phytoplankton productivity during upwelling-induced blooms, and also the small copepod species (e.g. *Acartia*) that are able to track the food increase at short time-scales. In turn, the abundance of small copepods and phytoplankton can be used efficiently by sardine through filter-feeding. On the other side, a growing influence of subtropical climate components, as indicated by EA, would increase water surface temperature and the stratification of the surface layer, while the average intensity of upwelling and its frequency decreases. Phytoplankton productivity would decrease because of the reduced nutrient input, but changes in the dominance of species (i.e. dinoflagellates vs. diatoms) or local blooms caused by changes in currents may lead to increases in biomass (Richardson and Schoeman, 2004). Reduced upwelling would be a positive factor for anchovy recruitment and large copepods, which are able to feed on relatively large phytoplankton, such as some dinoflagellates. Also, adult anchovy would find food of appropriate size and produce large reproductive output.

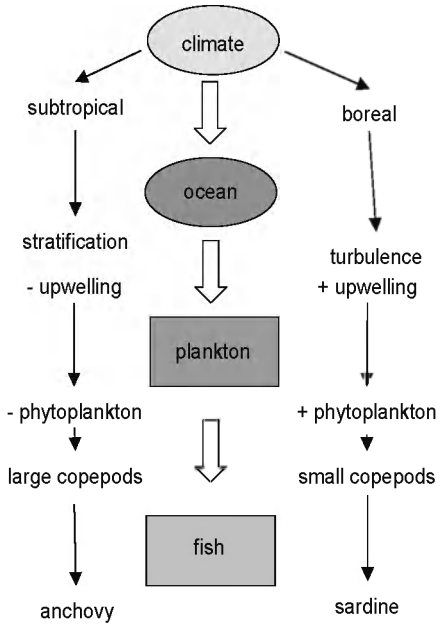

Figure 6.1. Conceptual model linking changes in climate to those in the ocean and ecosystem components at a regional scale in northwestern Iberia and the Bay of Biscay. (ICES, 2007.)

The conceptual model described in Figure 6.1 describes the average multi-annual dynamics in the main climate, oceanographic, and ecological features in the study region. However, the conditions leading to alternative states of the ecosystem are different from those proposed for other upwelling regions (e.g. van der Lingen *et al.*, 2006). One possible explanation for such a difference is the nature of the main direct external forcing on the ecosystem, in this case, the upwelling. Being a marginal upwelling area within the large Northeast Atlantic upwelling region, the northwest Iberian shelf has upwelling events of much shorter duration and intensity than those in areas located to the south (e.g. northwest Africa or southern Benguela). In this context, relative anomalies of upwelling intensity or frequency within a particular region may represent very different energy inputs in absolute value than upwelling regions. Also, reduced upwelling and increased stratification need to be viewed in relative terms, because upwelling events never cease completely. Subregional analysis may reveal the exact mechanisms triggering the biological response at each site, adding local complexity to the processes depicted in the model shown in Figure 6.1. An example of the interaction of factors at climate, biogeographic, and local scales was provided for the North Sea by Beaugrand (2004).

6.3 Regime shifts

The underlying causes for the variability described may also change during the observational period. This is suggested by the match and mismatch of positive and negative anomaly periods when comparing indices (e.g. Figure 5.6). Sudden changes in most series, such as those observed in the late 1970s, are generally associated with shifts in the oceanographic and ecosystem regimes (De Young *et al.*, 2004). Similar shifts were recognized in most upwelling regions (Borges *et al.*, 2003; Chavez *et al.*, 2003; Alheit and Niquen, 2004; Cury and Shannon, 2004). Large changes in climate related to the *El Niño*–Southern Oscillation (ENSO) were often claimed as one of the major underlying causes of ecosystem shift, mainly in the Pacific (Chavez *et al.*, 2003), but it can affect other oceans too, through climate teleconnections (Barnston and Livezey, 1987). Major changes in the ecosystems of the Northeast Atlantic have been

described for the period between the late 1970s and 1990, but the exact timing of the shift varied among target variables (Beaugrand, 2004; Edwards and Richardson, 2004; Richardson and Schoeman, 2004). Climate effects such as the change in windspeed and direction in the late 1970s may need different time to integrate as a clear response in some biological compartments. In this regard, plankton and short-lived pelagic fish are among the first to show change, but the ability to identify the timing also depends on the statistics employed (Beaugrand, 2004).

The shift in the late 1970s identified in this study coincides with a major ENSO-related shift in the Pacific (Chavez *et al.*, 2003; Alheit and Niquen, 2004), which is also indicated in zooplankton CPR data from the Northeast Atlantic (Dickson *et al.*, 1988; Richardson and Schoeman, 2004). One major feature of the shift detected in the Iberian case is the coincidence of peak abundance of both sardine and anchovy prior to 1975. Fishery data report a marked decrease in the distribution area of Iberian anchovy, formerly well distributed through the shelf (Junquera, 1984), but now restricted to major populations in the eastern Bay of Biscay and the Gulf of Cádiz (ICES, 2005). In contrast, sardine populations have fluctuated in abundance, but never abandoned their main centres of distribution (Carrera and Porteiro, 2003; ICES, 2005). The continued operation of upwelling, even reduced by global trends, and the decrease in suitable prey for anchovy in the region may explain the lack of success of anchovy in most parts of the region after 1980. Only appropriate conditions at local scales, such as the moderate upwelling and the existence of thermohaline fronts in the eastern Bay of Biscay (Borja *et al.*, 1998; Allain *et al.*, 2001) would allow maintenance of the species despite the average negative conditions in the region. Changes in the region considered in this study in the early 1990s were similar to those described in the Pacific (Chavez *et al.*, 2003) and were also found at subregional scales (Borges *et al.*, 2003). This fact supports a major role for teleconnection patterns at multidecadal scales, causing abrupt changes in the relationships between environmental and biological variables.

7 References

Alheit, J., and Niquen, M. 2004. Regime shifts in the Humboldt Current ecosystem. Progress in Oceanography, 60: 201–222.

Alheit, J., Möllmann, C., Dutz, J., Kornilovs, G., Loewe, P., Mohrholz, V., and Wasmund, N. 2005. Synchronous ecological regime shifts in the central Baltic and the North Sea in the late 1980s. ICES Journal of Marine Science, 62: 1205–1215.

Allain, G., Petitgas, P., and Lazure, P. 2001. The influence of mesoscale ocean processes on anchovy (*Engraulis encrasicolus*) recruitment in the Bay of Biscay, estimated with a three-dimensional hydrodynamic model. Fisheries Oceanography, 10: 151–163.

Ambar, I., and Howe, M. R. 1979. Observations of the Mediterranean Outflow – I. Mixing in the Mediterranean Outflow. Deep Sea Research, 26A: 535–554.

Arístegui, J., Álvarez-Salgado, X. A., Barton, E. D., Figueiras, F. G., Hernández-León, S., Roy, C., and Santos, A. M. P. 2004. Oceanography and fisheries of the Canary Current/Iberian region of the eastern North Atlantic. *In* The Sea. 14. The Global Coastal Ocean: Interdisciplinary Regional Studies and Syntheses, pp. 877–931. Ed. by A. R. Robinson and K. H. Brink. Harvard University Press, Cambridge, MA, USA.

Barnston, A. G., and Livezey, R. E. 1987. Classification, seasonality and persistence of low-frequency atmospheric circulation patterns. Monthly Weather Review, 115: 1083–1126.

Barton, E. D. 1998. Eastern boundary of the North Atlantic: Northwest Africa and Iberia coastal segment. *In* The Sea. 11. The Global Coastal Ocean, pp. 633–657. Ed. by A. R. Robinson and K. H. Brink. John Wiley and Sons, New York.

Beaugrand, G. 2004. The North Sea regime shift: evidence, mechanisms and consequences. Progress in Oceanography, 60: 245–262.

Bertrand, A., Segura, M., Gutiérrez, M., and Vásquez, L. 2004. From small-scale habitat loopholes to decadal cycles: a habitat-based hypothesis explaining fluctuation in pelagic fish populations off Peru. Fish and Fisheries, 5: 296–316.

Blanton, J. O., Atkinson, L. P., Fernández de Castillejo, F., and Lavín, A. 1984. Coastal upwelling off the Rías Bajas, Galicia, Northwest Spain. 1. Hydrographic studies. Rapports et Procès-Verbaux des Réunions du Conseil International pour l'Exploration de la Mer, 183: 79–90.

Bode, A., Alvarez-Ossorio, M. T., Carrera, P., and Lorenzo, J. 2004. Reconstruction of trophic pathways between plankton and the North Iberian sardine (*Sardina pilchardus*) using stable isotopes. Scientia Marina, 68: 165–178.

Bode, A., Alvarez-Ossorio, M. T., Cabanas, J. M., Porteiro, C., Ruiz-Villarreal, M., Santos, M. B., Bernal, M., *et al*. 2006. Recent changes in the pelagic ecosystem of the Iberian Atlantic in the context of multidecadal variability. ICES Document CM 2006/C:07. 18 pp.

Borges, M. F., Santos, A. M., Crato, N., Mendes, H., and Mota, B. 2003. Sardine regime shifts off Portugal: a time series analysis of catches and wind conditions. Scientia Marina, 67(Suppl. 1): 235–244.

Borja, Á., Uriarte, A., Valencia, V., Motos, L., and Uriarte, A. 1996. Relationships between anchovy (*Engraulis encrasicholus*) recruitment and the environment in the Bay of Biscay. Scientia Marina, 60(Suppl. 2): 179–192.

Borja, Á., Uriarte, A., Egaña, J., Motos, L., and Valencia, V. 1998. Relationship between anchovy (*Engraulis encrasicolus* L.) recruitment and environment in the Bay of Biscay (1967–1996). Fisheries Oceanography, 7: 375–380.

Botas, J. A., Fernández, E., Bode, A., and Anadón, R. 1990. A persistent upwelling off the central Cantabrian Coast (Bay of Biscay). Estuarine, Coastal and Shelf Science, 30: 185–199.

Bryden, H. L., Longworth, H. R., and Cunningham, S. A. 2005. Slowing of the Atlantic meridional overturning circulation at 25°N. Nature, 438: 655–657.

Buffaz, L., and Planque, B. 2006. Application of operational oceanography to fisheries management: the case of the anchovy in the Bay of Biscay. ICES Document CM 2006/E:02.

Cabanas, J. M. 2000. Variabilidad temporal en las condiciones oceanográficas de las aguas de la plataforma continental gallega. Algunas consecuencias biológicas. PhD thesis, Universidade de Vigo, 2000.

Carrera, P., and Porteiro, C. 2003. Stock dynamic of the Iberian sardine (*Sardina pilchardus*, W.) and its implication on the fishery off Galicia (NW Spain). Scientia Marina, 67: 245–258.

Chavez, F. P., Ryan, J., Lluch-Cota, S. E., and Ñiquen, M. C. 2003. From anchovies to sardines and back: multidecadal change in the Pacific Ocean. Science, 299: 217–221.

Conkright, M. E., Locarnini, R. A., Garcia, H. E., O'Brien, T. D., Boyer, T. P., Stephens, C., and Antonov, J. I. 2002. World Ocean Atlas 2001: Objective Analyses, Data Statistics and Figures. CD-ROM Documentation. NODC Internal Report 17, Silver Spring, MD. USA. 17 pp. 3 CD-ROMs available at http://www.nodc.noaa.gov/General/NODC-cdrom.html#woa01.

Cunha, M. E., Garrido, S., and Pissarra, J. 2005. The use of stomach fullness and colour indices to assess *Sardina pilchardus* feeding. Journal of the Marine Biological Association of the UK, 85: 425–431.

Curry, J. A., and Webster, P. J. 1999. Thermodynamics of the Atmospheres and Oceans. International Geophysics Series, 65. Academic Press, San Diego, CA. 471 pp.

Curry, R. G., and McCartney, M. S. 2001. Ocean gyre circulation changes associated with the North Atlantic Oscillation. Journal of Physical Oceanography, 31: 3374–3400.

Cury, P., and Shannon, L. J. 2004. Regime shifts in upwelling ecosystems: observed changes and possible mechanisms in the northern and southern Benguela. Progress in Oceanography, 60: 223–243.

De Young, B., Harris, R., Alheit, J., Beaugrand, G., Mantua, N., and Shannon, L. 2004. Detecting regime shifts in the ocean: data considerations. Progress in Oceanography, 60: 143–164.

Dickson, R. R., Kelly, P. M., Colebrook, J. M., Wooster, W. S., and Cushing, D. H. 1988. North winds and production in the eastern North Atlantic. Journal of Plankton Research, 10: 151–169.

Edwards, M., and Richardson, A. J. 2004. Impact of climate change on marine pelagic phenology and trophic mismatch. Nature, 430: 881–884.

Estrada, M., Vives, F., and Alcaraz, M. 1985. Life and productivity in open seas. *In* The Western Mediterranean, pp. 150–199. Ed. by R. Margalef. Pergamon Press, London.

Fernández, E., Cabal, J., Acuña, J. L., Bode, A., Botas, A., and García-Soto, C. 1993. Plankton distribution across a slope current-induced front in the southern Bay of Biscay. Journal of Plankton Research, 15: 619–641.

Fernández de Puelles, M. L., Valencia, J., and Vicente, L. 2004a. Zooplankton variability and climatic anomalies from 1994 to 2001 in the Balearic Sea (Western Mediterranean). ICES Journal of Marine Science, 61: 492–500.

Fernández de Puelles, M. L., Valencia, J., Jansá, J., and Morillas, A. 2004b. Hydrographical characteristics and zooplankton distribution in the Mallorca Channel (Western Mediterranean). ICES Journal of Marine Science, 61: 654–666.

Fiúza, A. F. G., de Macedo, M. E., and Guerreiro, M. R. 1982. Climatological space and time variation of the Portuguese coastal upwelling. Oceanologica Acta, 5: 31–40.

Font, J., Salat, J., and Tintoré, J. 1988. Permanent features of the circulation in the Catalan Sea. Oceanologica Acta, 9: 51–57.

Fraga, F. 1981. Upwelling off the Galician Coast, Northwest Spain. *In* Coastal Upwelling, pp. 176–182. Ed. by F. A. Richards. American Geophysical Union, Washington, DC.

Frouin, R., Fiúza, A. F. G., Ambar, I., and Boyd, T. J. 1990. Observations of a poleward surface current off the coasts of Portugal and Spain during winter. Journal of Geophysical Research, 95: 679–691.

García, E., Tintoré, J., Pinot, J. M., Font, J., and Manriquez, M. 1994. Surface circulation and dynamic of the Balearic Sea. Seasonal and interannual variability of the western Mediterranean Sea. Coastal and Estuarine Studies, 46: 73–91.

González-Pola, C., and Lavín, A. 2003. Oceanographic variability in the northern shelf of the Iberian coast. ICES Marine Science Symposia, 219: 71–79.

González-Pola, C., Lavín, A., and Vargas-Yáñez, M. 2005. Intense warming and salinity modification of intermediate water masses in the southeastern corner of the Bay of Biscay for the period 1992–2003. Journal of Geophysical Research, 110: 5–20.

González-Quirós, R., Cabal, J., Alvarez-Marqués, F., and Isla, A. 2003. Ichthyoplankton distribution and plankton production related to the shelf break front at the Avilés Canyon. ICES Journal of Marine Science, 60: 198–210.

Guisande, C., Cabanas, J. M., Vergara, A. R., and Riveiro, I. 2001. Effect of climate on recruitment success of Atlantic Iberian sardine *Sardina pilchardus*. Marine Ecology Progress Series, 223: 243–250.

Guisande, C., Vergara, A. R., Riveiro, I., and Cabanas, J. M. 2004. Climate change and abundance of the Atlantic–Iberian sardine (*Sardina pilchardus*). Fisheries Oceanography, 13: 91–101.

Hansen, J. L. S., Nazarenko, L., Ruedy, R., Sato, M., Willis, J., Del Genio, A., Koch, D., *et al.* 2005. Earth's energy imbalance: confirmation and implications. Science, 308: 1431–1435.

Hare, S. R., and Mantua, N. J. 2000. Empirical evidence for North Pacific regime shifts in 1977 and 1989. Progress in Oceanography, 47: 103–146.

Haynes, R., and Barton, E. D. 1990. A poleward flow along the Atlantic coast of the Iberian Peninsula. Journal of Geophysical Research, 95: 11425–11441.

Hunter, J. R., and Alheit, J. 1995. International GLOBEC small pelagic fishes and climate change program. GLOBEC Report, 8. 72 pp.

Hurrell, J. W. 1995. Decadal trends in the North Atlantic Oscillation: regional temperature and precipitation. Science, 269: 676–679.

Hurrell, J. W., and Dickson, R. R. 2004. Climate variability over the North Atlantic. *In* Marine Ecosystems and Climate Variation – the North Atlantic, pp. 15–31. Ed. by N. Ch. Stenseth, G. Ottersen, J. W. Hurrell, and A. Belgrano. Oxford University Press, Oxford.

ICES. 2005. Report of the ICES Advisory Committee on Fishery Management, Advisory Committee on the Marine Environment and Advisory Committee on Ecosystems, 2005, Volume 7. ICES Advice. Volumes 1–11. International Council for the Exploration of the Sea, Copenhagen. 1418 pp.

ICES. 2007. Report of the ICES/GLOBEC Workshop on Long-term Variability in SW Europe (WKLTVSWE), 13-16 February 2007, Lisbon, Portugal. ICES CM 2007/LRC:02. 111 pp.

Junquera, S. 1984. The anchovy fishery (*Engraulis encrasicholus*) in the Bay of Biscay and Atlantic Galician coasts since 1920. Quantitative variations. Revue des Travaux de l'Institut des Peches Maritimes Nantes, 48: 133–142.

Kerr, R. A. 2000. Globe's "missing warming" found in the ocean. Science, 287: 2126–2127.

Koutsikopoulos, C., Beillois, P., Leroy, C., and Taillefer, F. 1998. Temporal trends and spatial structures of the sea surface temperature in the Bay of Biscay. Oceanologica Acta, 21: 335–344.

Lavín, A., Díaz del Río, G., Cabanas, J. M., and Casas, G. 1991. Afloramiento en el noroeste de la Península Ibérica. Índices de afloramiento en el punto 43°N 11°W período 1966–1989. Informes Técnicos del Instituto Español de Oceanografía, 91: 1–40.

Lavín, A., Valdés, L., Sánchez, F., Abaunza, P., Forest, A., Boucher, J., and Lazure, P. 2005. The Bay of Biscay: the encountering of the ocean and the shelf. *In* The Sea. 14. The Global Coastal Ocean: Interdisciplinary Regional Studies and Syntheses, pp. 935–1002. Ed. by A. R. Robinson and K. H. Brink. Harvard University Press, Cambridge, MA, USA.

Lluch-Cota, D. B., Hernández-Vázquez, S., and Lluch-Cota, S. E. 1997. Empirical investigation on the relationship between climate and small pelagic global regimes and *El Niño*–Southern Oscillation (ENSO). FAO Fisheries Circular, 934.

Lopez-Jurado, J. L. 2002. Interannual variability in waters of the Balearic Islands. *In* Tracking Long-Term Hydrological Change in the Mediterranean Sea. CIESM Workshop Series, 16 (Special issue): 33–36.

Mantua, N. J. 2004. Methods for detecting regime shifts in large marine ecosystems: a review with approaches applied to North Pacific data. Progress in Oceanography, 60: 165–182.

Mason, E., Coombs, S. H., and Oliviera, P. 2006. An overview of the literature concerning the oceanography of the eastern North Atlantic region. Relatórios Científicos e Técnicos, Instituto Portugues de Investigacao Maritima, Série digital, 33. Available online at http://sabella.mba.ac.uk/1795/.

Mendes, H., and Borges, M. F. 2006. A sardinha no século XX: capturas e esforço de pesca. Relatórios Científicos e Técnicos, Instituto Portugues de Investigacao Maritima, Série digital, 32. Available online at http://www.inrb.pt/fotos/editor2/ipimar/rct.serie_digital/reln32final.pdf.

OSPAR. 2000. Quality Status Report 2000. Region IV – Bay of Biscay and Iberian Coast. OSPAR Commission, London. 134 pp.

Peliz, A., Rosa, T. L., Santos, A. M. P., and Pissarra, J. L. 2002. Fronts, jets and counter-flows in the western Iberian upwelling system. Journal of Marine Systems, 35: 61–77.

Peliz, A., Dubert, J., and Haidvogel, D. B. 2003a. Subinertial response of a density-driven eastern boundary poleward current to wind forcing. Journal of Physical Oceanography, 33: 1633–1650.

Peliz, A., Dubert, J., Haidvogel, D. B., and Le Cann, B. 2003b. Generation and unstable evolution of a density-driven eastern poleward current: the Iberian poleward current. Journal of Geophysical Research, 108(C8): 3268, doi:10.1029/2002JC001443.

Peliz, A., Dubert, J., Santos, A. M. P., Oliveira, P. B., and Le Cann, B. 2005. Winter upper ocean circulation in the western Iberian Basin – fronts, eddies and poleward flows: an overview. Deep Sea Research Part I – Oceanographic Research Papers, 52: 621–646.

Pérez, F. F., Ríos, A. F., King, B. A., and Pollard, R. T. 1995. Decadal changes of the Θ–S relationship of the Eastern North Atlantic Central Water. Deep Sea Research I, 42: 1849–1864.

Pérez, F. F., Pollard, R. T., Read, J. F., Valencia, V., Cabanas, J. M., and Ríos, A. F. 2000. Climatological coupling of the thermohaline decadal changes in Central Water of the eastern North Atlantic. Scientia Marina, 64: 347–353.Pingree, R. D. 1993. Flow of surface waters to the west of the British Isles and in the Bay of Biscay. Deep Sea Research, 40: 369–388.

Pingree, R. D., and Le Cann, B. 1990. Structure, strength and seasonality of the slope currents in the Bay of Biscay region. Journal of the Marine Biological Association of the UK, 70: 857–885.

Pinot, J. M., Tintore, J., and Gomis, D. 1994. Quasi-synoptic mesoscale variability in the Balearic Sea. Deep Sea Research, 41: 897–914.

Pinot, J. M., Lopez Jurado, J. L., and Riera, M. 2002. The Canales experiment (1996–1998). Interannual seasonal and mesoscale variability of the circulation in the Balearic channels. Progress in Oceanography, 55: 325–370.

Planque, B., Jegou, A. M., Beillois, P., Lazure, P., Petitgas, P., and Puillat, I. 2003. Large scale hydrodynamic variability in the Bay of Biscay: the 1990s in the context of the interdecadal changes. ICES Marine Science Symposia, 219: 333–336.

Relvas, P., Barton, E. D., Dubert, J., Oliveira, P. B., Peliz, A., da Silva, J. C., and Santos, A. M. P. 2006. Physical oceanography of the western Iberian Ecosystem: latest views and challenges. Progress in Oceanography, 74: 149–173.

Richardson, A. J., and Schoeman, D. S. 2004. Climate impact on plankton ecosystems in the Northeast Atlantic. Science, 305: 1609–1612.

Ríos, A. F., Pérez, F. F., and Fraga, F. 1992. Water masses in the upper and middle North Atlantic Ocean east of the Azores. Deep Sea Research, 39: 645–658.

Ruiz-Villarreal, M., González-Pola, C., Díaz del Río, G., Lavín, A., Otero, P., Piedracoba, S., and Cabanas, J. M. 2006. Oceanographic conditions in North and Northwest Iberia and their influence on the *Prestige* oil spill. Marine Pollution Bulletin, 53: 220–238.

Santos, A. M. P., Peliz, A., Dubert, J., Oliveira, P. B. O., Angélico, M. M., and Ré, P. 2004. Impact of a winter event on the distribution and transport of sardine (*Sardina pilchardus*) eggs and larvae off western Iberia: a retention mechanism. Continental Shelf Research, 24: 149–165.

Schwartzlose, R. A., Alheit, J., Bakun, A., Baumgartner, T. R., Cloete, R., Crawford, R. J. M., Fletcher, W. J., *et al.* 1999. Worldwide large-scale fluctuations of sardine and anchovy populations. South African Journal of Marine Science, 21: 289–347.

Serra, N., and Ambar, I. 2002. Eddy generation in the Mediterranean undercurrent. Deep Sea Research II, 49: 4225–4243.

Siedler, G., Church, J., and Gould, J. 2001. Ocean circulation and climate: observing and modelling the global ocean. International Geophysics Series, 77. Academic Press, San Diego, CA. 715 pp.

Stenseth, N. Ch., Mysterud, A., Ottersen, G., Hurrell, J. W., Chan, K-S., and Lima, M. 2002. Ecological effects of climate fluctuations. Science, 297: 1292–1296.

Uriarte, A., Roel, B. A., Borja, Á., Allain, G., and O'Brien, C. M. 2002. Role of environmental indices in determining the recruitment of the Bay of Biscay anchovy. ICES Document CM 2002/O:25. 32 pp.

Valdés, L., López-Urrutia, A., Cabal, J., Alvarez-Ossorio, M., Bode, A., Miranda, A., Cabanas, M., *et al.* 2007. A decade of sampling in the Bay of Biscay: what are the zooplankton time series telling us? Progress in Oceanography, 74: 98–114.

Valencia, V., Borja, Á., Fontán, A., Pérez, F. F., and Ríos, A. F. 2003. Temperature and salinity fluctuations in the Basque Coast (southeastern Bay of Biscay), from 1986 to 2000, related to the climatic factors. ICES Marine Science Symposia, 219: 340–342.

Valencia, V., Franco, J., Borja, Á., and Fontán, A. 2004. Hydrography of the southeastern Bay of Biscay. *In* Oceanography and Marine Environment of the Basque Country, pp. 159–194. Ed. by Á. Borja and M. Collins. Elsevier Oceanography Series, 70.

van der Lingen, C. D., Hutchings, L., and Field, J. G. 2006. Comparative trophodynamics of anchovy *Engraulis encrasicolus* and sardine *Sardinops sagax* in the southern Benguela: are species alternations between small pelagic fish trophodynamically mediated? African Journal of Marine Science, 28: 465–477.

Villamor, B., González-Pola, C., Lavín, A., Valdés, L., Lago de Lanzós, A., Franco, C., Cabanas, J. M., *et al.* 2005. Distribution and survival of larvae of mackerel (*Scomber scombrus*) in the North and Northwest of the Iberian Peninsula, in relation to environmental conditions during spring 2000. ICES Document CM 2004/J:07. 34 pp.

Von Storch, H., and Zwiers, F. W. 1999. Statistical Analysis in Climate Research. Cambridge University Press, Cambridge. 484 pp.

Wooster, W. S., Bakun, A., and McLain, D. R. 1976. The seasonal upwelling cycle along the eastern boundary of the North Atlantic. Journal of Marine Research, 34: 131–140.

Author contact information

Jürgen Alheit
Leibniz Institute for Baltic Sea Research
Seestrasse 15
18119 Rostock, Germany
juergen.alheit@io-warnemuende.de

Antonio Bode
Instituto Español de Oceanografía (IEO)
Paseo Marítimo Alcalde Francisco Vázquez, 10
15001 A Coruña, Spain
antonio.bode@co.ieo.es

Maria de Fátima Borges
Instituto Português do Mar e da Atmosfera (IPMA)
Avenida de Brasília
1449-006 Lisbon, Portugal
mfborges@ipma.pt

Mª Luz Fernández de Puelles
Instituto Español de Oceanografía (IEO)
Centro Oceanográfico de Baleares
Muelle de Poniente, s/n
07015 Palma de Mallorca, Spain
mluz.fernandez@ba.ieo.es

Louize Hill
Rue de Hennin 53
1050 Brussels, Belgium
louize.hill@yahoo.co.uk

Alicia Lavín
Instituto Español de Oceanografía (IEO)
Prom. San Martin s/n
39080 Santander, Spain
alicia.lavin@st.ieo.es

Hugo Mendes
Instituto Português do Mar e da Atmosfera (IPMA)
Avenida de Brasília
1449-006 Lisbon, Portugal
hmendes@ipma.pt

Manuel Ruiz-Villarreal
Instituto Español de Oceanografía (IEO)
Paseo Marítimo Alcalde Francisco Vázquez, 10
15001 A Coruña, Spain
manuel.ruiz@co.ieo.es

A. Miguel P. Santos
Instituto Português do Mar e da Atmosfera (IPMA)
Avenida de Brasília
1449-006 Lisbon, Portugal
amsantos@ipma.pt

Raquel Somavilla
Instituto Español de Oceanografía (IEO)
Prom. San Martin s/n
39080 Santander, Spain
raquel.somavilla@st.ieo.es

Andrés Uriarte
Centro Tecnológico del Mar y los Alimentos (AZTI)
Herrera Kaia, Portua
20110 Pasaia, Spain
auriarte@pas.azti.es

Victor Valencia
Centro Tecnológico del Mar y los Alimentos (AZTI)
Herrera Kaia, Portua
20110 Pasaia, Spain
vvalencia@pas.azti.es

Manuel Vargas-Yáñez
Instituto Español de Oceanografía (IEO)
Centro Oceanografico de Málaga
29640 Fuengirola, Spain
manolo.vargas@ma.ieo.es

List of abbreviations

See also the list of abbreviations of variables in Section 3.

ACF	autocorrelation factor
ACA	*Acartia* abundance
ACI	*Acartia–Calanus* index
AIW	Atlantic Intermediate Water
CAL	*Calanus*
CLI	climatic indices
COP	total copepod abundance
CPR	Continuous Plankton Recorder
e.d.f.	effective degrees of freedom
ENACW	Eastern North Atlantic Central Water
ENACWP	Eastern North Atlantic Central Water of subpolar origin
ENACWT	Eastern North Atlantic Central Water of subtropical origin
ENSO	*El Niño*–Southern Oscillation
ICOADS	International Comprehensive Ocean–Atmosphere Dataset
MOW	Mediterranean Outflow Water
MW	Mediterranean Water
OCE	oceanographic indices
PC	principal component
PCA	principal component analysis
PCI	phytoplankton colour index
SAHFOS	Sir Alister Hardy Foundation for Ocean Science
SHF	sensible heat flux
SST	sea surface temperature
WIBP	Western Iberia Buoyant Plume
ZMF	zonal momentum flux